## *The Relationship between CO2 and Ubiquitin in the NF-κB Signalling Pathway*

THOMAS, MICHAEL,JAMES

# The Relationship between $CO_2$ and Ubiquitin in the NF-κB Signalling Pathway

This thesis is submitted for the degree of
Master of Science by Research

Michael James Thomas

Department of Biosciences
Durham University
2018

## Abstract

Carbon dioxide ($CO_2$) forms a significant proportion of the earth's atmosphere and plays a crucial role in a number of biological processes including photosynthesis, respiration and acid-base homeostasis. While $CO_2$ is generally unreactive, at physiological temperatures and pressures it is capable of combining rapidly with neutral amines to form carbamates. Moreover, protein carbamylation has been implicated in the induction of subtle conformational changes, eliciting effects within cellular systems and thus functioning as a post-translational modification (PTM). While the labile and readily-reversible nature of this reaction has hindered the study of carbamylation modifications, technological developments continue to facilitate investigations. The ability to chemically trap carbamates under physiologically relevant conditions, for example, has resulted in the identification of ubiquitin as a candidate for modification by carbamylation.

The ubiquitin system has been implicated in a range of biological processes, from gene expression to mediating the stress response. However, it has been demonstrated to play a particularly significant role in the selective degradation of intracellular proteins. Moreover, the ubiquitin-dependent degradation of proteins is involved in the regulation of numerous biological processes, notably the NF-κB signalling pathway. Canonical activation of NF-κB signalling has been shown to be regulated by the K48-linked polyubiquitination-dependent degradation of IκB, a family of inhibitory proteins.

This thesis provides insight into the relationship between $CO_2$ and ubiquitin in NF-κB signalling. Under physiologically high concentrations of $CO_2$, inhibition of K48-linked polyubiquitination was observed, in addition to a reduction in the degradation of IκBα. Furthermore, use of a transcriptional reporter cell line demonstrated a $CO_2$-mediated suppression of NF-κB signalling, in concordance with existing reports. Transfecting cells with a K48R mutant demonstrated the substantial role had by the K48 residue in the regulation of NF-κB signalling, as hypothesised. Overall, this thesis offers a more comprehensive understanding of the ubiquitin-dependent regulation of NF-κB signalling, and the sensitivity of this mechanism to $CO_2$ and carbamylation.

## Declaration

The work presented in this thesis was carried out at Durham University between October 2017 and September 2018. The work is my own original research unless otherwise indicated by statement or citation. This work has not been submitted for any other qualification.

## Statement of copyright



## Acknowledgements

First and foremost I wish to thank my supervisor Professor Martin Cann for his endless support and optimism throughout my project. I would like to thank Dr Victoria Linthwaite for her guidance and relentless questioning of my ability, as well as the members of Lab 234 for making my year so enjoyable. Thanks Mum, Dad, Philip, Auntie Lu and Rebecca for your constant support and willingness to spend time in the same room as me.

# Contents

# Abbreviations

| | |
|---|---|
| 1,3-BPG | 1,3-bisphosphoglycerate |
| 3-PG | 3-phosphoglycerate |
| ALI/ARDS | Acute lung injury/acute respiratory distress syndrome |
| BSA | Bovine serum albumin |
| CA | Carbonic anhydrase |
| CHX | Cyclohexamide |
| $CO_2$ | Carbon dioxide |
| COPD | Chronic obstructive pulmonary disease |
| Cx26 | Connexin 26 |
| Da | Dalton |
| DMEM | Dulbecco's modified eagle medium |
| DMSO | Dimethyl sulfoxide |
| *E. coli* | *Escherichia coli* |
| FBS | Fetal bovine serum |
| G3P | Glyceraldehyde 3-phosphate |
| $H^+$ | Protons |
| Hb | Haemoglobin |
| HEK 293 | Human embryonic kidney cells 293 |
| IKK | IκB kinase |
| K | Lysine |
| KO | Knockout |
| LB | Lysogeny broth |
| NF-κB | Nuclear factor-κB |
| NLS | Nuclear localisation sequence |
| PBS | Phosphate-buffered saline |
| PenStrep | Penicillin-streptomycin antibiotic |
| PTM | Post-translational modification |
| R | Arginine |
| rt | Room temperature |
| RuBisCO | Ribulose bisphosphate carboxylase oxygenase |
| SDS-PAGE | Sodium dodecyl sulphate polyacrylamide gel electrophoresis |
| TEO | Triethyloxonium tetrafluoroborate |
| TNF | Tumour necrosis factor |
| TNFR | Tumour necrosis factor family |
| TRAF | TNFR-associated factor |
| UV | Ultraviolet |
| VILI | Ventilator-induced lung injury |
| WT | Wild-type |

# List of schemes



# List of figures

# Chapter 1: Introduction

## 1-1 Overview

The research presented within this thesis is an investigation into the relationship between $CO_2$ and ubiquitin in the context of the NF-κB signalling pathway.

Previous work has highlighted the functionality of $CO_2$ in mediating the carbamate PTM. The nucleophilic attack of a neutral amine on $CO_2$ to form a carbamate has been demonstrated to contribute to the regulation of certain proteins. While carbamates have been previously understudied due to the labile and reversible nature of this reaction, technological developments including the ability to chemically trap carbamylated proteins under physiologically relevant conditions have facilitated investigations into this modification.

Proteomic screening for new protein carbamates has identified ubiquitin as a candidate for modification by carbamylation. Ubiquitination is a widespread biological regulatory system involved in the control of major processes, including cell-cycle progression, receptor regulation and signalling pathways such as the NF-κB signalling pathway, a key regulator of innate immunity and inflammation.

Overall, this work aims to provide insight into the relationship between $CO_2$ and ubiquitin, and is intended to provide a greater understanding of how certain physiological symptoms observed in patients suffering from elevated blood $pCO_2$ (termed hypercapnia) may be a result of increased carbamylation and its effect on ubiquitin's role as a regulator of NF-κB signalling, and the subsequent downstream effects.

This chapter aims to provide a general overview of $CO_2$ and carbamylation's role as a PTM. The significance of the ubiquitin system and its involvement in NF-κB signalling will be discussed in the context of specific medical observations made from patients who exhibit hypercapnia.

## 1-2 Physiology of $CO_2$ and its role in biological systems

$CO_2$ has a fundamental role in all aspects of biological systems through its effects on photosynthesis, respiration and acid-base homeostasis (Hetherington and Raven, 2005; Gutkneckt *et al*., 1977; Joshi and Tabita, 1996). This is facilitated by the hydrophobic properties of $CO_2$, enabling its hydration and the formation of carbonic acid. In solution, carbonic acid rapidly dissociates into bicarbonate ions and protons (Scheme 1-1). The concentration of $CO_2$ in a cell therefore directly correlates to cellular pH (Blombach and Takors, 2015).

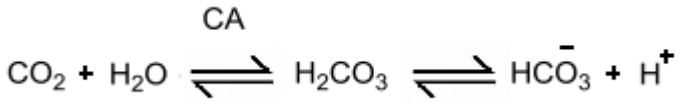


**Scheme 1-1 The equilibria between the hydration of $CO_2$ to bicarbonate. The equilibria between $CO_2$ and carbonic acid by carbonic anhydrase and the rapid dissociation of carbonic acid to bicarbonate ions and protons.**

### 1-2.1 Carbonic anhydrase

Hydration of $CO_2$ to form carbonic acid occurs relatively slowly at physiological pH and therefore functions as the rate-limiting step in the equilibrium shown in Scheme 1-1 (Kalifah, 1973). This hydrating step is, in turn, catalysed by carbonic anhydrases (CAs), a group of enzymes with high turnover rates of up to approximately 1 million molecules of $CO_2$ per second (Lindskog, 1997; Frommer, 2010). The significance of CAs in biological processes is evidenced by the fact that they have been so well evolutionarily conserved amongst Archaea, prokaryotes and eukaryotes (Supuran *et al*., 2003). This infers that sensing and responding to changes in $CO_2$ as well as the associated changes in cellular pH is an important mechanism.

## 1-3 Carbamylation and its role as a post-translational modification

A mechanism by which $CO_2$ regulates biological processes is via its direct interactions with particular proteins. While $CO_2$ is generally unreactive, it is capable of combining directly with amines under physiologically relevant temperatures, pressures and pH to form carbamates. Carbamylation is a result of the nucleophilic attack of neutral amines on $CO_2$ (Hampe and Rudkevich, 2003) and results in the conversion of a side chain lysine or *N*-terminal residue from basic/neutral to acidic (Lorimer and Miziorko, 1980). A schematic of this reaction is demonstrated in Scheme 1-2.

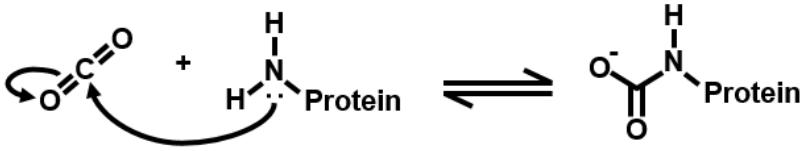


**Scheme 1-2 The nucleophilic attack of a neutral amine on $CO_2$ to form a carbamate.**

Carbamylation-induced modification of a protein's amino acid charge status can therefore induce conformational changes in peptide structure or binding which ultimately, may prompt changes within a cellular system (Terrier and Douglas, 2010).

The formation of carbamates, however, is a labile and readily reversible reaction. This, in turn, has resulted in carbamylation being a difficult modification to study (Jimenez-Morales *et al*., 2014). In acidic conditions the carboxyl group is released, rendering the detection of the modification difficult via mass spectrometry. Despite this, the role of carbamylation is understood in a number of target proteins, including Haemoglobin, Connexin 26 and RuBisCO, (Terrier and Douglas, 2010; Meigh *et al*., 2013; Lorimer and Miziorko, 1980) which will be discussed in greater detail later in the chapter. Moreover, further developments in experimental methods have allowed for better studying of carbamate formation and its target proteins. For example, Linthwaite developed a method for trapping carbamates under physiologically relevant pH and $CO_2$ concentration by ethyl esterification with the electrophilic Meerwein reagent triethyloxonium tetrafluoroborate (TEO) (Linthwaite *et al*.,

2018). The trapped carbamate is stabilised and can be detected using mass spectrometry.

Advancements such as this have begun to expand our understanding of the range of proteins whose functions are modified by carbamate formation; the number of proteins whose functions are potentially regulated by carbamylation is constantly increasing, suggesting that this modification is a far more widespread regulatory system than previously anticipated.

### 1-3.1 Examples of carbamylated proteins

While the identification of carbamylation-mediated proteins is ongoing, a number of proteins whose functions are dependent on carbamylation are already well understood.

#### 1-3.1.1 Haemoglobin

Haemoglobin (Hb) represents one of the first proteins to be identified, whose function is modified through carbamylation. Hb is a highly characterised protein, with its role in the transport of oxygen in red blood cells being well-defined. The binding properties between Hb and oxygen, and therefore the ability of Hb to transport oxygen, is altered by the binding of $CO_2$ (Terrier and Douglas, 2010). An increase in blood $pCO_2$ induces a decrease in the binding affinity of Hb to oxygen, resulting in the dissociation of oxygen from Hb. This phenomenon is termed the Bohr Effect, and is facilitated by the binding of $CO_2$ to neutral *N*-terminal amino groups of Hb chains, producing carbaminohaemoglobin (Hsia, 1998). Experimental work identified that $CO_2$ binds preferentially to the $\beta$ chains of Hb as opposed to $\alpha$ chains (Kilmartin *et al*., 1973; Matthew *et al*., 1977). It is significant to note that approximately 10-20% of transport of $CO_2$ in the blood is achieved by Hb via this mechanism (Vandegriff *et al*., 1991).

#### 1-3.1.2 Connexin 26

Gap junctions have a vital role in the direct cell-cell transfer of ions and small molecules (Goodenough and Paul, 2009). Gap junctions are composed of two hemichannels, which are formed primarily by connexin proteins (Meigh *et al*., 2015). Connexin 26 (Cx26) forms a hemichannel that has been demonstrated to be sensitive to changes in $CO_2$, most likely as a result of carbamate

formation on its Lysine 125 (K125) residue (Meigh *et al*., 2013). In this study, genetic manipulations of the K125 residue of Cx26 demonstrated that carbamylation of K125 is required for Cx26 activation. The increased channel activity was demonstrated to be a result of increased $CO_2$ levels, and was independent of associated changes in pH.

### 1-3.1.3 RuBisCO

$CO_2$ has a critical role in plant biology via its involvement in photosynthesis; $CO_2$ functions as the substrate for the carbon-fixing enzyme ribulose bisphosphate carboxylase-oxygenase (RuBisCO) (Raines, 2003), one of the most abundant proteins on earth. Moreover, carbon fixation constitutes a significant component of the light-independent reactions of photosynthesis, otherwise termed the Calvin cycle, as shown in Figure 1-1.

The Calvin cycle has a fundamental role in the generation of precursor molecules required by plants for growth (Raines, 2003). In photosynthesis, $CO_2$ is fixed to ribulose 1,5 bisphosphate by the carbon fixing enzyme RuBisCO. Due to the instability of the six-carbon molecule produced, it is quickly metabolised to two molecules of 3-phosphoglycerate (3-PG). One 3-PG molecule is phosphorylated by phosphoglycerate kinase, resulting in the production of 1,3-biphospoglycerate (1,3-BPG), while the other 3-PG molecule is released. 1,3-BPG is in turn reduced by glyceraldehyde 3-phosphate dehydrogenase to form glyceraldehyde 3-phosphate (G3P), five molecules of which are used in the regeneration of three molecules of ribulose 1,5 bisphosphate. The remaining molecules of G3P are used in the generation of glucose (Raines, 2003).

Significantly, RuBisCO represents the first enzyme known to be activated by carbamate formation, in addition to utilising $CO_2$ as a substrate (Lorimer, 1979). The correct function of RuBisCO is entirely dependent upon the formation of a carbamate on a lysine residue within the enzyme's active site. This site is distinct from the binding site of substrate $CO_2$ (Lorimer, 1979); X-ray crystallography identified the required carbamate formation site as the lysine 201 (K201) of RuBisCO (Miziorko, 1979).

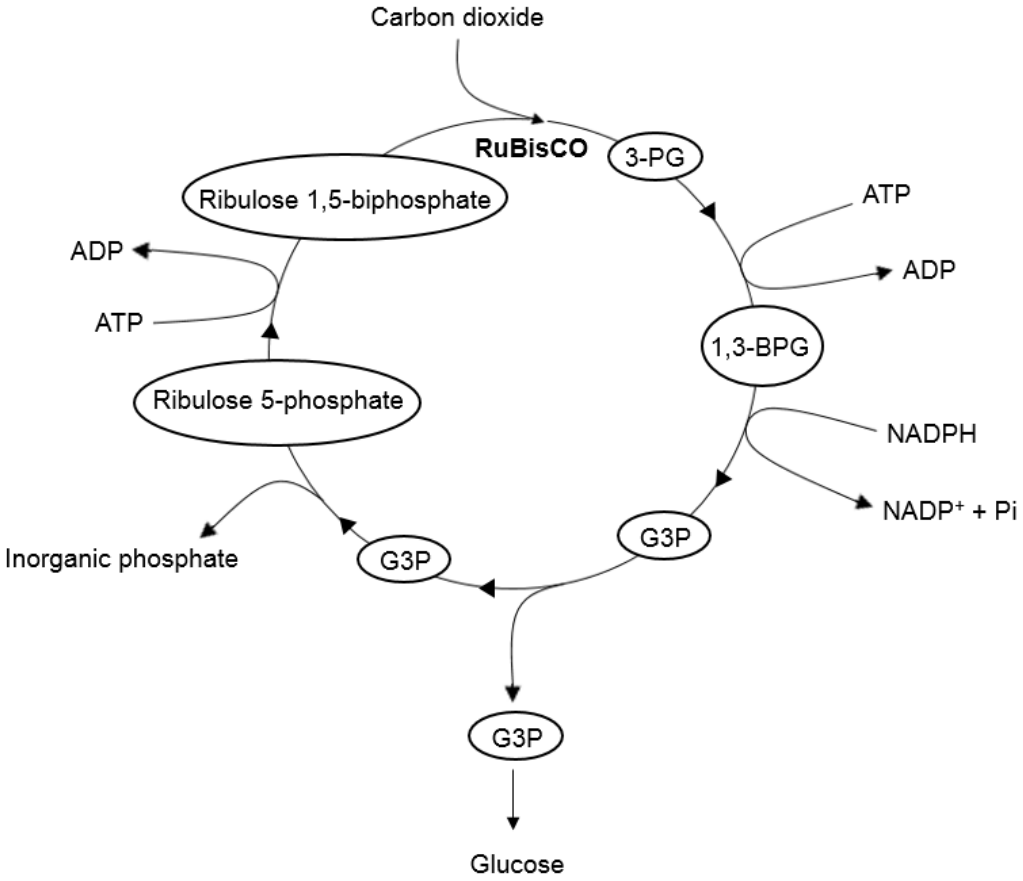


**Figure 1-1 The Calvin cycle. The fixation of $CO_2$ by RuBisCO, the reduction of 1-BPG to G3P and the regeneration of ribulose 1,5-bisphosphate. Molecules of G3P are utilised in the generation of molecules important for growth.**

## 1-4 Ubiquitin and its role as a regulatory system

### 1-4.1 Ubiquitin as a candidate for post-translational modification by carbamylation

Ubiquitin is a highly conserved, 8.5 kDa, 76-amino acid polypeptide that is present universally throughout the eukaryotic kingdom (Hershko and Ciechanover, 1998). The ubiquitin system has been implicated in a number of significant biological processes within the cell, ranging from the control of gene expression to mediating stress responses (Hershko and Ciechanover, 1998). Moreover, the ubiquitin system has been demonstrated to have a particularly important role in the selective degradation of intracellular proteins via the 26S proteasome, an ATP-dependent protease (Schwarts and Ciechanover, 1992). The function of the ubiquitin system is facilitated by the protein's seven lysine residues. Interestingly, a proteomic screen for new protein carbamates identified their formation at the lysine 48 (K48) residue of ubiquitin (Linthwaite, 2017). As discussed in the context of known carbamylated proteins, carbamylation can induce significant changes in protein conformation and function, eliciting an impact on downstream processes.

### 1-4.2 Mechanism of protein ubiquitination

#### 1-4.2.1 Signalling for protein ubiquitination

Signalling for a protein to be targeted by ubiquitination has been shown to be achieved primarily by three mechanisms: genetic programming, protein phosphorylation or spontaneous damage. The ubiquitination of a number of proteins has been demonstrated to be dependent upon a short sequence of amino acids within their structure (Wilkinson, 2000). Alternatively, the phosphorylation of a number of proteins, including IκBα, β-catenin, p53 and JunI has been shown to be crucial for their ubiquitination (Laney and Hochstrasser, 1999). The ubiquitination of damaged proteins often functions as a signal for degradation via the 26S proteasome. Moreover, it is hypothesised that ubiquitination of spontaneously damaged proteins is a result of their misfolded structure, an assumption based on the fact that misfolded proteins found in the endoplasmic reticulum are translocated to the cytoplasm via retrograde transport and degraded in a ubiquitin-dependent manner (Plemper and Wolf, 1999).

### 1-4.2.2 The biochemistry of ubiquitin conjugation

The conjugation of ubiquitin to its protein substrates is typically dependent upon the function of three enzymes (Wilkinson, 2000): the E1 activating enzyme, the E2 ubiquitin-conjugating enzyme, and the E3 ubiquitin ligase. These enzymes, as well as ATP, are critical to the function of the ubiquitin system and ultimately facilitate the covalent conjugation of ubiquitin to its target protein (Haas and Siepmann, 1997). This process is demonstrated in Figure 1-2.

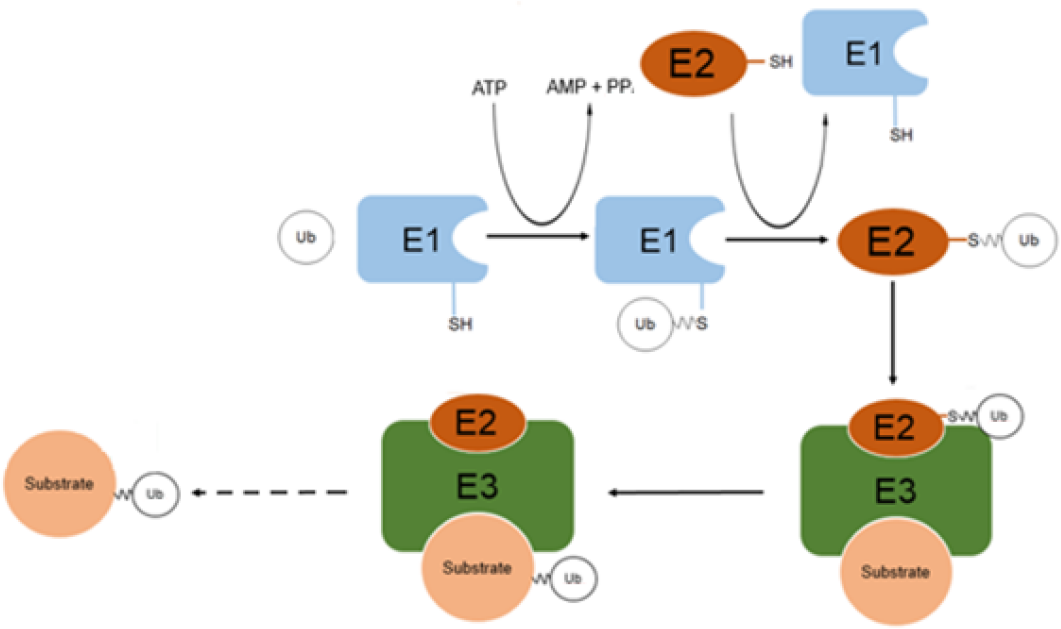


**Figure 1-2 The biochemistry of ubiquitin conjugation. Ubiquitin conjugation to its target substrate is reliant on the function of the E1 activating enzyme, the E2 ubiquitin-conjugating enzyme and the E3 ubiquitin ligase, as well as ATP.**

### 1-4.2.3 The biological role of polyubiquitination

While the initial conjugation of ubiquitin to its target substrate is crucial to the function of the ubiquitin system, the significance of ubiquitination as a regulatory system throughout biological processes is dependent on the subsequent conjugation of multiple, additional ubiquitin molecules. This is termed polyubiquitination (Li and Ye, 2008). The conjugation of these additional, consecutive ubiquitin molecules occurs via the molecules' seven lysine residues: K6, K11, K27, K33, K48 and K63 (Sadowski *et al*., 2011). The multitude of potential sites per ubiquitin molecule on which polyubiquitination can occur permits the formation of a number of different structures. In turn, the

polyubiquitin structure formed can function as a signal for the protein's fate (Sadowski *et al*., 2011). Furthermore, previous work has demonstrated that polyubiquitin chains formed by different linkage types are involved in conveying unique functional information about the ubiquitin-conjugated protein (Li and Ye, 2008). For example, polyubiquitination via the K33 residue has been linked to regulation of cell surface receptor-mediated signal transduction (Huang *et al*., 2010). Alternatively, K63-linked polyubiquitination has been implicated in ribosomal biogenesis and DNA repair (Li and Ye, 2008). It has been demonstrated that polyubiquitination through the K48 residue, in particular, is involved in signalling for protein degradation of the tagged protein via the 26S proteasome, an ATP-dependent, large multi-protein complex that functions as a protease (Mallette and Richard, 2012; Bedford *et al*., 2010).

## 1-5 The molecular basis of the NF-κB signalling pathway

The Nuclear factor (NF)-κB signalling pathway poses a significant and attractive area of research due to the extensive number of genes under its control, as well as the unique nature by which it is regulated (Karin, 1999a). NF-κB signalling has been widely implicated in a number of processes, including the regulation of proinflammatory genes such as cytokines and chemokines, the regulation of context-dependent apoptosis and the regulation of energy homeostasis via the engagement of cellular networks governing glycolysis and respiration (Lawrence, 2009; Lin *et al*., 1999; Tornatore *et al*., 2012). As a result, it remains one of the best-characterised and well-understood signalling pathways, both in its regulation and its downstream effects. Despite the role of NF-κB signalling in a number of biological processes, its activity in cells of the immune system has been particularly highlighted due to its significant involvement in inflammation and innate immunity (Mathes *et al*., 2008; Dev *et al*., 2010). It is thus unsurprising that understanding the function and regulation of the NF-κB signalling pathway is considered a top priority among researchers within the biomedical field.

The mammalian NF-κB family is composed of five members including RelA, RelB, c-Rel, p50, and p52 (Sun, 2010). These proteins exhibit highly conserved DNA-binding and dimerisation domains, enabling the formation of homo- and heterodimers (Serasanambati and Chilakapati, 2016). Moreover, the extent of conservation within these domains has resulted in most members of the NF-κB family being theoretically able to form dimers (Siebenlist *et al*., 1994). The formation of dimeric complexes is crucial to NF-κB transcription factor function, with different dimer subunit combinations exhibiting variable nucleo-cytoplasmic subcellular localisation (Sun, 2010). While under non-activated conditions, NF-κB proteins remain sequestered in the cytoplasm. In the nucleus, NF-κB transcription factor dimers bind to 9-10 base pair DNA sites (termed κB sites), eliciting a change in the expression of target genes (Hayden and Ghosh, 2012).

Activation NF-κB signalling is regulated by two distinct pathways: the canonical and non-canonical pathways (Karin, 1999b; Senftleben, 2001). While

differences between the canonical and non-canonical activation pathways of NF-κB signalling exist, activation of both pathways is dependent upon the function of the proteasome (Sun, 2010). It is the mechanism by which the transcription factors are released that distinguishes between the category of signalling (Karin, 1999a).

Non-canonical activation of the NF-κB signalling pathway is dependent on the proteasomal processing of p100 and p105 precursor proteins to the functionally active p50 and p52 proteins (Sun, 2010). The proteasome-mediated processing of both p105 and p100 not only facilitates the ability of p50 and p52 to form dimers and induce changes in the expression of target genes, but has also been shown to disrupt the inhibitory function of p105 and p100 (Sun and Ley, 2008).

Alternatively, canonical activation of the NF-κB signalling pathway is dependent on the degradation of inhibitory IκB proteins via the 26S proteasome. The activity of NF-κB signalling in this pathway is therefore tightly regulated through interactions with members of the inhibitory protein family IκB (Hoesel and Schmid, 2013). Under non-activated conditions, IκB forms numerous interactions with NF-κB, which physically mask the nuclear localisation sequence (NLS) of the given NF-κB dimer, thus inhibiting its ability to translocate to the nucleus (Chen and Ghosh, 1999). Canonical activation of the NF-κB signalling pathway is a result of IκB kinase (IKK)-mediated phosphorylation-induced degradation of IκB molecules (Shih *et al*., 2010). Liberation of NF-κB dimers from IκB reveals the NLS, enabling the translocation of NF-κB dimers to the nucleus, where the expression of target genes is induced (Hoesel and Schmid, 2013).

Previous work has demonstrated that the canonical activation-induced degradation of the IκB inhibitor via the 26S proteasome is dependent on the function of the ubiquitin system (Mathes *et al*., 2012). Furthermore, K48-linked polyubiquitination has been previously implicated in signalling for the selective degradation of intracellular proteins, and was found to be directly responsible for regulation of NF-κB activation (Ohtake *et al*., 2016). Induction of the NF-κB signalling pathway induces the phosphorylation and activation of the IKK

complex, in turn resulting in the phosphorylation of the IκB inhibitor (Chen and Ghosh, 1999). This phosphorylation signals for subsequent K48-linked polyubiquitination, and ultimately degradation of the IκB inhibitor via the 26S proteasome (Ohtake *et al*., 2016). Overall, this work highlights the importance of K48-linked polyubiquitination-dependent protein degradation in the regulation of NF-κB signalling.

## 1-6 Hypercapnia-mediated inflammatory and immune suppression

It has been established in the above that the NF-κB signalling pathway has a significant role in the regulation of inflammation and innate immunity through the expression of target genes (Mathes *et al*., 2008; Dev *et al*., 2010). Furthermore, K48-linked polyubiquitination-dependent protein degradation of the IκB family of inhibitory molecules has been shown to regulate canonical activation of NF-κB signalling (Ohtake *et al*., 2016). Significantly, the ubiquitin system has been identified as a potential candidate for PTM by carbamylation at the K48 residue (Linthwaite, 2017).

It is therefore interesting to note that patients suffering from elevated blood $pCO_2$ (> = approximately 50 mmHg) termed hypercapnia (Costello *et al*., 1997), a result of several lung pathologies such as chronic obstructive pulmonary disease (COPD) and acute lung injury/acute respiratory distress syndrome (ALI/ARDS), also suffer from symptoms including a reduced inflammatory response and inhibited innate immunity, as well as an increased susceptibility to bacterial infection (Ohtake *et al*., 2016; Helenius *et al*., 2009). Mechanical ventilation strategies that induce high tidal volumes have been shown to induce further lung injury, termed ventilator-induced lung injury (VILI), and are typically avoided as a therapeutic treatment (Chonghaile *et al*., 2005). On the other hand, despite the benefits of low-lung stretch ventilator strategies in reducing mechanical trauma, the resultant induction of permissive hypercapnia has been associated with an active role in pathogenesis of inflammation (Chonghaile *et al*., 2005). Moreover, an increase in immunosuppression and the promotion of bacterial growth has been observed in response to the induction of hypercapnia (Marhong and Fan, 2014).

These observations are supportive of the hypothesis that under conditions of physiologically high $CO_2$ concentrations, carbamate formation induces a modification in the functionality of the ubiquitin system, a key regulator of inflammation and innate immunity via NF-κB signalling. Moreover, it infers that the symptoms observed in hypercapnic patients, primarily a reduced inflammatory response and inhibited innate immunity, are due to the $CO_2$-

mediated suppression of NF-κB signalling, which is likely caused by the inhibition of K48-linked polyubiquitination-dependent degradation of the IκB inhibitors.

Supportive of this idea, previous studies have highlighted a number of changes in molecular components involved in the ubiquitin-dependent regulation of NF-κB signalling in response to $CO_2$. In response to *in vitro* buffered hypercapnic conditions, an increase in nuclear IKK was observed, alongside a decrease in IκB degradation (Cummins *et al*., 2010). Such changes would, in turn, result in a decrease in the ability of NF-κB dimers to translocate to the nucleus and induce the expression of target genes due to the masking of the NLS by non-degraded IκB (Keogh *et al*., 2017). This theory has been supported through the use of a luciferase promoter reporter downstream of NF-κB target genes, which demonstrated an overall decrease in NF-κB signalling in response to increased $CO_2$ levels (Cummins *et al*., 2010). The significance of this has been further emphasised by *in vitro* assays inducing hypercapnic acidosis in A549 lung epithelial cells and pulmonary endothelial cells. It was observed that in response to the hypercapnic acidosis, there was a reduction in the ubiquitin-dependent degradation of IκB and, in turn, a decrease in NF-κB signalling (O'Toole *et al*., 2009; Cummins *et al*., 2010; Takeshita *et al*., 2003).

## 1-7 Motivation for investigation

The functionality of $CO_2$ as a PTM via its interactions with amino groups has been found to have a significant role in a number of biological processes, most notably in respiration and photosynthesis via physical interactions with Hb and RuBisCO. Further advancements in experimental methods have facilitated the study of carbamates as a PTM. Proteomic screens, for example, have begun to suggest that the number of proteins whose function is regulated by $CO_2$ is greater than previously anticipated. In addition to this, computational methods have suggested that up to as many as 1.3% of proteins may be carbamylated to some degree (Jimenez-Morales *et al*., 2014).

Previous work has identified ubiquitin as a target for carbamylation at its K48 residue (Linthwaite, 2017). The ubiquitin system represents a widespread regulatory system that is universal across eukaryotes and has been implicated in major processes including the control of inflammation and innate immunity via the regulation of the NF-κB signalling pathway (Mathes *et al*., 2008; Dev *et al*., 2010).

An investigation into the relationship between $CO_2$ and ubiquitin will enable a greater understanding of how carbamylation of ubiquitin functions as a PTM. This study intends to provide insight in to how carbamylation of ubiquitin can elicit effects on major downstream processes such as NF-κB signalling.

### 1-7.1 Project relevance

The practical relevance of this project arises from the clinical and medical implications associated with $CO_2$ mechanisms of action. Normal blood $pCO_2$ levels are essential for cellular function and are maintained within the body via homeostasis (Meigh *et al*., 2013). However, several lung pathologies including COPD and ALI/ARDS induce a reduced ventilatory ability and, in turn, increased blood $pCO_2$. Furthermore, non-invasive palliative artificial ventilation strategies are often utilised as treatments for such lung pathologies, which induce permissive hypercapnia. It has been hypothesised that permissive $CO_2$-mediated immune suppression may be a possible therapy in the tolerance of metabolic stress (Laffey *et al*., 2004). Patients suffering from hypercapnia

often exhibit additional symptoms including a reduced inflammatory response and inhibited innate immunity (Ohtake *et al*., 2016; Dev *et al*., 2010). In addition, increased $CO_2$ concentration has been linked to inhibited NF-κB signalling, a key regulator of inflammation and immunity (O'Toole *et al*., 2009). It is possible that the medical observations made from patients suffering from hypercapnia are a result of the effect of increased blood $pCO_2$ on the ubiquitin-dependent regulation of NF-κB signalling. This project was therefore aimed at providing insight into this possibility.

### 1-7.2 Aims and hypotheses

The overarching hypothesis of this project states that in response to an increase in $CO_2$ concentration, a suppression in NF-κB signalling will be observed. It was further hypothesised that the $CO_2$-mediated suppression of NF-κB signalling is a result of carbamylation-induced modification of the K48 residue of ubiquitin, in turn inhibiting the ability to undergo K48-linked polyubiquitination. As discussed, K48-linked polyubiquitination in particular has been implicated in the selective degradation of intracellular proteins via the 26S proteasome, and has been demonstrated to directly regulate the selective degradation of IκB, a family of inhibitors which mask the NF-κB dimer's NLS. It was hypothesised that a $CO_2$-mediated inhibition of K48-linked polyubiquitination would inhibit the degradation of IκB, eliciting an increased sequestration of NF-κB dimers within the cytoplasm. This, in turn, would prevent the translocation of NF-κB dimers into the nucleus, ultimately inhibiting the expression of target genes.

# Chapter 2: Materials and Methods

## 2-1 Materials and Equipment

All materials were purchased from Sigma-Aldrich unless otherwise stated.

### 2-1.1 Cell lines

*Escherichia coli* (*E. coli*) DH5α (non-antibiotic-resistant) cells were used for all DNA manipulation work. Human embryonic kidney cells 293 (HEK 293) acquired from Professor Martin Cann (Durham University) were used for mammalian cell assay work. A NF-κB/293/GFP-Luc Transcriptional Reporter Cell Line (System Biosciences) provided by Dr Eoin Cummins (University of Dublin) was used for quantification of NF-κB signalling. A human glioblastoma astrocytoma NF-κB/U251/GFP-Luc Transcriptional Reporter Cell Line provided by Dr Darius Widera (University of Reading) was also used for quantification of NF-κB signalling.

### 2-1.2 Plasmids

Plasmid DNA was purchased from Addgene unless otherwise stated.

### 2-1.3 Antibodies

Antibodies were purchased from Abcam unless otherwise stated.

## 2-2 Molecular Biology

### 2-2.1 Bradford assay

Samples with known protein concentrations were made with bovine serum albumin (BSA) ranging from 0 mg/mL to 10 mg/mL in 1x phosphate-buffered saline (PBS) or 1x Lysis Buffer. Bradford reagent 1x (250 µL) was added to 5 µL of sample and incubated for 5 min at room temperature (rt). The absorbance was measured at 595 nm using a Synergy™ H4 Hybrid Multi-Mode Microplate Reader. The measurements were plotted to generate a standard curve. This curve could then be used to measure unknown sample protein concentrations within this range.

### 2-2.2 Transforming cells

Plasmid DNA (2 µL, 50 ng/µL) was added to ultra-competent DH5α cells (40 µL). The solution was incubated on ice for 20 min. The solution was then heat shocked at 42 °C for 45 s and placed back on ice for 2 min. Lysogeny broth (LB) (900 µL) was added and the cells were incubated with shaking at 37 °C for 1 h. The culture was then centrifuged at 6,000 xg for 5 min and the pellet resuspended in LB (100 µL). Resuspended (100 µL) pellet was spread on an LB agar plate containing antibiotics specific to the cell line and plasmids, and incubated at 37 °C overnight. Plates were removed from the incubator 18 h later and stored at 2 – 8 °C.

### 2-2.3 Overnight culture growth

Overnight cultures between 5 mL to 50 mL LB were inoculated with a plate colony and the culture incubated with shaking at 37 °C overnight in the presence of antibiotics as appropriate.

### 2-2.4 Miniprep of overnight cultures

Minipreps were carried out using a Spin Miniprep Kit (QIAGEN). An overnight LB culture (5 mL) was centrifuged for 5 min at 4,200 xg and the supernatant removed. The pellet was resuspended in resuspension buffer (250 µL), and transferred to a microcentrifuge tube. Lysis solution (250 µL) was added and the tube inverted 3 – 4 times, before being incubated for 2 min. Neutralisation buffer was added (350 µL) and the tube inverted 4 – 6 times. The mixture was

then centrifuged at 13,000 xg for 5 min and the supernatant transferred to a spin column. This was centrifuged for 1 min and the flow through discarded. Wash solution (500 µL) was added, the column centrifuged, the flow through discarded, and then repeated with an empty column to remove residual solution. The column was transferred to a fresh collection tube and incubated with $dH_2O$ (50 µL) for 20 min at rt. The column was centrifuged for 2 min at 13,000 xg to collect the DNA.

### 2-2.5 Miraprep of overnight cultures

A modification of the Spin Miniprep Kit protocol was used to achieve larger yields of DNA, similar to that achieved by a Spin Maxiprep Kit, termed Miraprep (Pronobic *et al*., 2016). Overnight LB culture (50 mL) was centrifuged at 4,200 xg for 5 min and the supernatant removed. The pellet was resuspended in resuspension buffer (2 mL). Lysis solution (2 mL) was added and the tube inverted 3 – 4 times. Neutralisation buffer (2 mL) was added and the tube inverted 3 – 4 times. Lysate was distributed into 1.5 mL Eppendorf tubes by pouring. The lysate was spun at 13,200 xg for 10 min. Supernatant was collected in a single falcon tube (15 mL). Ethanol (96%) (5 mL) was added to the supernatant, and mixed. The sample-ethanol mix was loaded into spin-columns, and spun for 30 s at 13,200 xg. Wash solution (500 µL) was added, the column centrifuged, the flow through discarded, and then repeated with an empty column to remove residual solution. The column was transferred to a fresh collection tube and incubated with $dH_2O$ (35 µL), at rt for 20 min and centrifuged for 2 min at 13,200 xg to collect the DNA. Nucleic acid quantitation was measured using a NanoDrop (ThermoFisher), and DNA was stored at -20 °C.

### 2-2.6 Agarose gel

Periodically, the quality of DNA produced from miniprep (section 2-2.4) and miraprep (section 2-2.5) protocols was examined via electrophoreses on a 1% (w/v) agarose gel. Agarose (1.0 g) was dissolved in TAE buffer (100 mL) and microwaved for 1 min. Ethidium bromide (0.1 mg) was added before the gel was poured and set. DNA samples were run (25 µL) on the gel at 120 V for 1 h with TAE buffer. Gels were visualised under UV transillumination.

### 2-2.7 SDS-PAGE gel

Protein molecular weights were assessed using sodium dodecyl sulphate polyacrylamide gel electrophoresis (SDS-PAGE) gel. Protein samples (10 or 30 µg, dependent upon experiment) were made up 1:1 in loading buffer (100 mM Tris-HCl pH 6.8, 200 mM dithiothereitol, 4% (w/v) SDS, 0.2% (w/v) bromophenol blue, 20% (v/v) glycerol) and were incubated for 10 min at 95 °C to enable protein denaturation. The samples were run on resolving gels in the range 8% – 12% (w/v) with 5% stacking gel. A protein ladder (Pageruler$^{TM}$ pre-stained) was used to estimate protein size. The gels were run in running buffer (25 mM Tris-HCl pH 7.5, 192 mM glycine, 0.1% (w/v) SDS) at 150 V for 2 h. If intended for visualisation, the gel was incubated with Coomassie Brilliant Blue G (20 mL, 3 mM Coomassie Brilliant Blue G, 12 M methanol and 2 M glacial acetic acid) with rocking overnight. SDS-PAGE gels intended for Western blotting were not stained.

### 2-2.8 Western blot

Proteins were transferred from SDS-PAGE gels via electroblotting in transfer buffer (25 mM Tris, 190 mM glycine, 20% methanol, 0.25% (w/v) SDS) onto nitrocellulose membranes at 60 V for 18 h at 2 – 8 °C. Nitrocellulose membranes were blocked for 1 h with blocking buffer (2% non-fat dry milk in TBS-0.05% Tween 20), and incubated with the appropriate concentration of primary antibody diluted in 10 mL blocking buffer for 24 h at 2 – 8 °C. Specific antibody dilution is described below per assay. Membranes were washed with TBS-0.05% Tween 20 for 3 x 5 min, 1 x 15 min, 1 x 30 min, and incubated with horseradish peroxidase-conjugated secondary antibody for 1 h. Membranes were washed according to the above method, however the final 30 min wash contained no Tween 20. The membranes were treated with an ECL reagent (GE Healthcare Life Sciences) according to the manufacturer's instructions and the signals visualised using a chemiluminescent-sensitive CDC camera (BioRad).

### 2-2.9 Quantification of Western blots

Western blots were quantified using ImageJ software. Images were inverted to reduce background noise intensity. Using saved pre-set areas, the raw integrated density of the signals was measured.

## 2-3 Routine mammalian cell culture

All cell culture was carried out inside a sterile Class II biological safety cabinet to prevent contamination; cells were regularly monitored to assess wellbeing using light microscopy. The inside of the safety cabinet, as well as equipment and resources moving into the safety cabinet, were cleaned thoroughly using ethanol (70%). The cell lines used are described above (2-1.1).

### 2-3.1 Cell retrieval

Cells were cryopreserved at -150 ºC in Dulbecco's Modified Eagle medium (DMEM) (Fisher Scientific) supplemented with 10% fetal bovine serum (FBS) (Fisher Scientific), 1% Penicillin-Streptomycin antibiotic (PenStrep) (Fisher Scientific) and 10% dimethyl sulfoxide (DMSO). When required for cell retrieval, cells were rapidly thawed in a 37 °C water bath with gentle agitation for 2 min. Cells were transferred to 4 mL complete growth media (89% DMEM, 10% FBS and 1% PenStrep) in a canted neck, vented cap cell culture flask (T25) (Fisher Scientific). The cells were stored at 5% $CO_2$ and 37 °C under humidified conditions. The growth media was changed 24 h later to remove the DMSO. Growth media was changed every 48 h to prevent nutrient starvation and cell death.

### 2-3.2 Cell passaging

Cell cultures were enzymatically passaged once grown to 70-90% confluency to prevent senescence of the cell line and to seed cultures required for assays. Growth media was aspirated from the flask and cells were washed with 2 mL 1x PBS for 2 min at rt. Next, PBS was aspirated and cells were incubated for 5 – 15 min (dependent upon cell line) at 37 ºC, 5% $CO_2$ in 1 mL 0.05% Trypsin-EDTA (Fisher Scientific) to induce cellular detachment from plasticware. Gentle agitation following incubation with Trypsin-EDTA solution induced the full detachment of cells from plasticware. Cellular detachment was confirmed by observation under light microscopy. A further 5 min of incubation at 37 ºC and 5% $CO_2$ was conducted if full detachment was not observed. The cell suspension was diluted to the appropriate density through the addition of complete growth medium. Cells were mixed vigorously via pipetting to break clusters of cells and ensure an even distribution throughout the media. New

vented cap cell culture flasks (T25 and T75), as well as cell culture treated multidishes (6-well and 24-well) (Fisher Scientific) intended for assays were seeded at an appropriate density. Cells were grown at 5% $CO_2$ and 37 °C under humidified conditions. Growth media was changed every 48 h to prevent nutrient starvation and cell death.

## 2-4 Mammalian cell work

### 2-4.1 Toxicity assays

Determining the appropriate concentration and length of treatment of chemicals and compounds used in this study was deduced using toxicity assays. These assays utilise cell death/damage as a measure of toxicity.

The effect of increasing concentrations of treatment on cell viability was examined in order to determine an appropriate concentration. Cells were grown to 70 – 90% confluency and incubated with an increasing concentration of the treatment of interest for a predetermined duration. Cells were aspirated and resuspended in 1x PBS (150 µL). The cell suspension was diluted in a 1:1 ratio by the addition of 0.4% Trypan Blue (150 µL), and incubated for 5 min at rt. 5 µL of stained cells were pipetted onto a haemocytometer, and the number of live (white) cells and dead/damaged (blue) cells were counted in a predetermined area. The percentage of dead/damaged cells in that sample was calculated. The relationship between the concentration of treatment and the percentage of dead/damaged cells provided a measure by which to determine a suitable concentration for maximum potency while limiting cell death/damage.

Determining the appropriate length of treatment was achieved using a timescale assay. Cells were grown to 70 – 90% confluency and treated with a known concentration of treatment for an increasing amount of time, ranging from 0 h to 12 h. At each determined time point, media was aspirated from the cells, and the cells were resuspended in 1x PBS (150 µL). The cell suspension was diluted in a 1:1 ratio by the addition of 0.4% (w/v) Trypan Blue (150 µL) and incubated for 5 min at rt. 5 µL of stained cells were pipetted onto a haemocytometer, and the number of live (white) cells and dead/damaged (blue) cells were counted in a predetermined area. The percentage of dead/damaged cells in that sample was calculated. The relationship between duration of treatment and the percentage of dead/damaged cells provided a measure by which to determine a suitable duration of treatment.

It is important to note that while trypan exclusion may not fully equate to the death of a cell, it is a useful marker of cell damage and thus toxicity.

### 2-4.2 Mammalian cell transfection

Transfection of mammalian cells with DNA (section 2-2.4 and 2-2.5) was carried out using a Lipofectamine™ 3000 Transfection Reagent (Thermo Fisher Scientific) according to the manufacturer's instructions. Confirmation that this protocol was cell-line compatible was achieved by transfecting a group of cells with a GFP-encoding plasmid. Cells expressing GFP were visualised by fluorescence microscopy.

### 2-4.3 Assaying total protein per cell

HEK 293 cells were grown to 90% confluency and treated with 20 µg/mL cyclohexamide (CHX) at 5% $CO_2$ and 10% $CO_2$, 37 ºC, under humidified conditions for 18 h. 10% $CO_2$ was chosen to replicate arterial $CO_2$ concentrations associated with acute hypercapnia (Keogh *et al*., 2017). Cells were also treated to the above described conditions excluding 20 µg/mL CHX. Cells were aspirated and resuspended in 1x PBS (500 µL). Cell suspension (250 µL) was diluted in a 1:1 ratio by the addition of 0.4% (w/v) Trypan Blue (250 µL), and incubated for 10 min. A sample of stained cells (5 µL) were pipetted onto a haemocytometer, and the number of live (white) cells was counted in a predetermined area. The number of live cells per mL was calculated. The remaining cell suspension was lysed via sonication for 10 s. The cell lysate was centrifuged at 12,000 xg for 1 min, and the supernatant transferred to a new Eppendorf tube. The protein concentration of the lysate sample was measured through performing a Bradford assay as described using 5 µL of the lysate. The total protein per live cell was calculated using these values.

### 2-4.4 Assaying K48-linked polyubiquitination

HEK 293 cells were grown to 90% confluency and treated with 5% $CO_2$ and 10% $CO_2$, at 37 ºC, under humidified conditions for 18 h. Controls for the intracellular and extracellular pH changes associated with the transition from 5% $CO_2$ to 10% $CO_2$ were utilised. Controlling for the change in intracellular pH was achieved through the addition of 2 mM propionic acid (Cook *et al*., 2012), while controlling for the change in extracellular pH was achieved by the addition of media pre-set to pH 7.3. Cells were aspirated and resuspended in

1x PBS (300 µL). The cell suspension was lysed via sonication for 10 s, and centrifuged at 12,000 xg for 1 min. The protein content of the cell lysate was examined via Bradford assay (section 2-2.1). Samples were ran on an 8% SDS-PAGE gel (section 2-2.7) and electroblotted onto a nitrocellulose membrane (section 2-2.8). K48-linked polyubiquitination was assayed by Western blot (section 2-2.8) using an anti-ubiquitin (linkage-specific K48) primary monoclonal antibody in a 1:1,000 dilution. A loading control was utilised to remove error caused by unequal loading. Vinculin was assayed by Western blot (section 2-2.8) using an anti-vinculin primary antibody in a 1:5,000 dilution.

### 2-4.5 Assaying NF-κB activation

NF-κB/293/GFP-Luc and NF-κB/U251/GFP-Luc cells were grown to 90% confluency and treated with TNF-α ranging from 2 ng/mL to 100 ng/mL at 37 °C under conditions of 5% $CO_2$ and 10% $CO_2$ for 18 h. Cells were aspirated and lysed in 1x lysis buffer (300 µL) and centrifuged at 13,200 xg. A sample of cell lysate (200 µL) was pipetted to a black 96-well plate. GFP fluorescence intensity was measured from this sample through excitation/emission of wavelength 485/530 nm using a Synergy™ H4 Hybrid Multi-Mode Microplate Reader. Protein concentration of cell lysate was examined via Bradford assay (section 2-2.1). These values enabled the fluorescent counts per µg protein to be calculated.

### 2-4.6 Assaying IκBα degradation

HEK 293 cells were grown to 90% confluency and treated with 100 ng/mL TNF-α at 5% $CO_2$ and 10% $CO_2$, 37 ºC, under humidified conditions for 18 h. In later assays, a shorter, 3h duration of treatment was utilised to reduce the possibility of IκBα restoring to normal levels. Controls for both the intracellular and extracellular pH change associated with the transition from 5% $CO_2$ to 10% $CO_2$ were used, as described above (section 2-4.4). Cells were aspirated and resuspended in 1x PBS (300 µL). The cell suspension was lysed via sonication for 10 s, and centrifuged at 12,000 xg for 1 min. The protein content of the cell lysate was examined via Bradford assay (section 2-2.1). Samples were ran on a 12% SDS-PAGE gel (section 2-2.7) and electroblotted onto a nitrocellulose

membrane (section 2-2.8). IκBα was assayed by Western blot (section 2-2.8) using an anti-IκBα antibody in a 1:2,000 dilution. A loading control was utilised to remove error caused by unequal loading. Vinculin was assayed by Western blot (section 2-2.8) using an anti-vinculin primary antibody in a 1:5,000 dilution.

# Chapter 3: $CO_2$ and K48-linked polyubiquitination-dependent protein degradation

## 3-1 Overview

The functionality of $CO_2$ in mediating the carbamate PTM and the roles played by this modification in a number of biological processes have been discussed (section 1-3). The nucleophilic attack of neutral amines on $CO_2$ results in the electrostatic shift of a lysine side chain or *N*-terminal residue from basic/neutral to acidic (Lorimer and Miziorko, 1980), with a potential influence on protein conformation and function. Such changes in peptide structure or ligand binding may ultimately elicit changes within a cellular system (Terrier and Douglas, 2010).

Developments in chemical trapping alongside proteomic screening has aided the identification of carbamylated proteins (Linthwaite *et al*., 2018); a previous screen identified a carbamate on the lysine residue at position 48 (K48) in ubiquitin (Linthwaite, 2017). While the ubiquitin system has been implicated in a significant number of biological processes, ranging from the control of gene expression to the mediation of stress responses (Hershko and Ciechanover, 1998), it has been demonstrated to be particularly crucial in the selective degradation of intracellular proteins via the 26S proteasome (Schwarts and Ciechanover, 1992). Furthermore, previous work has highlighted the necessity of K48-linked polyubiquitination in signalling for protein degradation (Mallette and Richard, 2012). Consequently, carbamylation at this residue may elicit changes in the function of ubiquitin, with downstream effects on the selective degradation of intracellular proteins.

This thesis aims to investigate the relationship between $CO_2$ and ubiquitin-driven processes. The functionality of the ubiquitin K48 residue will form the central focus of this study on account of the advanced degree of understanding already established with regards to this particular lysine residue. In particular, the formation of a carbamate on the ubiquitin K48 residue is of significant interest: our current understanding indicates that carbamylation is able to induce conformational and functional changes in a protein (Terrier and Douglas, 2010), while K48-linked polyubiquitination is implicated in signalling

for the selective degradation of intracellular proteins (Mallette and Richard, 2012). Carbamylation at this site may therefore ultimately elicit an impact on processes regulated by K48-linked polyubiquitination-dependent protein degradation.

This chapter aims to investigate the relationship between $CO_2$ and K48-linked polyubiquitination-dependent protein degradation. The effect of $CO_2$ on K48-linked polyubiquitination was examined, alongside changes in total protein per cell.

## 3-2 Investigating the relationship between $CO_2$ and K48-linked polyubiquitination

For this work, increased cellular $CO_2$ concentrations are assumed to increase carbamate occupancy, although this remains to be formally proven. Subsequently, it was anticipated that $CO_2$-mediated carbamate formation on the K48 residue of ubiquitin would be more prevalent at elevated $CO_2$ concentrations. Moreover, it was hypothesised that carbamylation of ubiquitin's K48 residue, and the consequent shift in electrostatic charge status, would induce an impact on the protein's function. It was further hypothesised that carbamylation of ubiquitin at the K48 residue would inhibit K48-linked polyubiquitination.

### 3-2.1 Developing an assay to examine K48-linked polyubiquitination

In order to test the above hypotheses, an assay was developed, enabling the investigation of the effect of $CO_2$ on K48-linked polyubiquitination (section 2-4.4). HEK 293 cells, selected based on their reliable turnover and propensity for transfection, were incubated at 5% $CO_2$ and 10% $CO_2$ for 18 h, ensuring full gassing of the cell culture. Alternatively, assessing the rate of change in medium colour could have been utilised to measure the duration of incubation required for full gassing of the cell culture. Controls accounting for the intracellular and extracellular pH changes associated with the shift from 5% $CO_2$ to 10% $CO_2$ ensured that observed changes in K48-linked polyubiquitination were a result of the change in $CO_2$ concentration and not due to fluctuations in pH. Controlling for the change in extracellular pH was achieved by the addition of 7.3 pH media, while controlling for the change in intracellular pH was achieved through the addition of 2 mM propionic acid (Cook *et al*., 2012). Cells were lysed via sonication to release their cellular content for analysis, which was then separated via SDS-PAGE gel. An 8% SDS-PAGE gel was used to account for the large molecular weight of the K48-linked complexes; use of a higher percentage gel may have reduced the movement of K48-linked complexes, making them harder to visualise. The extent of K48-linked polyubiquitin was examined by Western blot, using a monoclonal anti-ubiquitin (linkage-specific K48) antibody. To prevent the

occurrence of experimental artefacts produced by unequal sample loading, a vinculin loading control was used. Calculating the relative intensity of the K48-linked polyubiquitination sample against the vinculin loading control produced a more reliable final assessment of the effect of $CO_2$ on polyubiquitin chain formation at K48.

### 3-2.2 $CO_2$-mediated inhibition of K48-linked polyubiquitination

Using the assay described (section 3-2.1), the effect of $CO_2$ on K48-linked polyubiquitination was examined. Figure 3-1 displays 3 replicates (I-III) of the Western blots produced from probing HEK 293 whole cell lysates with an anti-ubiquitin (K48-linkage specific) antibody and an anti-vinculin antibody, following their respective treatments. It can be observed that the signal intensity for K48-linked ubiquitin is significantly weaker at 10% $CO_2$ in comparison to 5% $CO_2$. Furthermore, the vinculin loading controls appear to

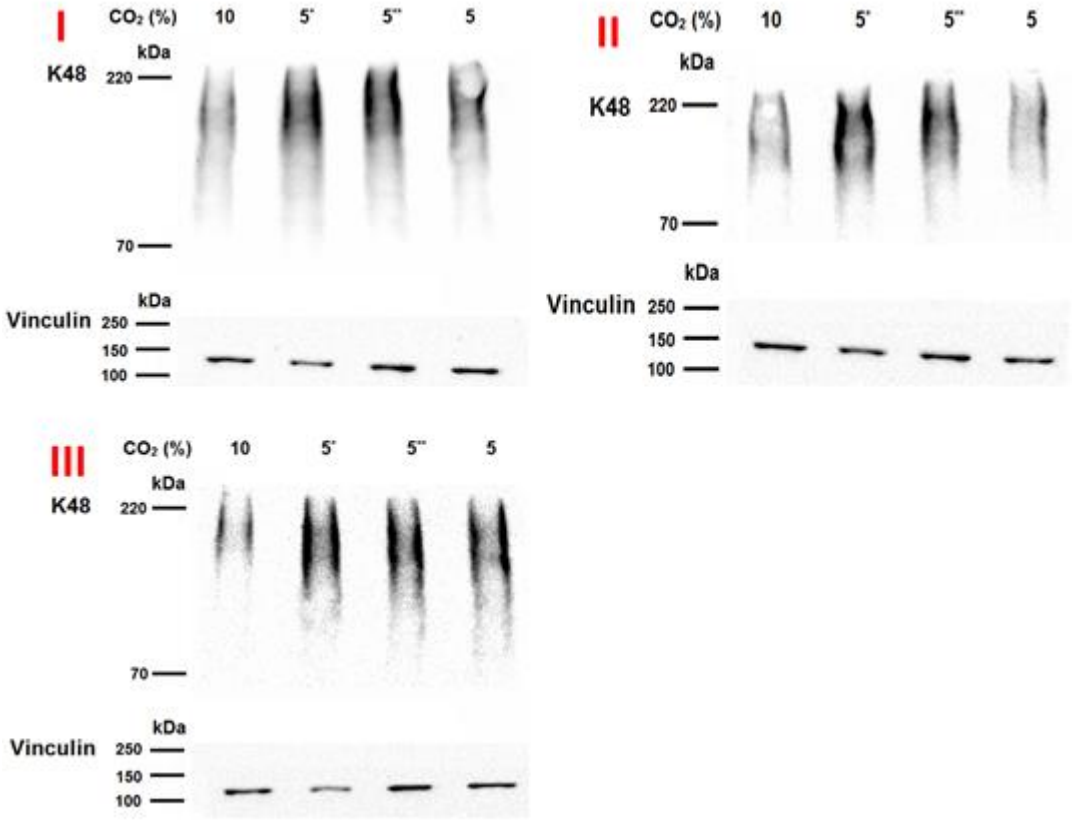


**Figure 3-1 The effect of $CO_2$ on K48-linked polyubiquitination. Western blot replicates (I-III) displaying the effect of $CO_2$ on K48-linked polyubiquitination (K48) and vinculin loading control signal intensity. * indicates extracellular pH control. ** indicates intracellular pH control.**

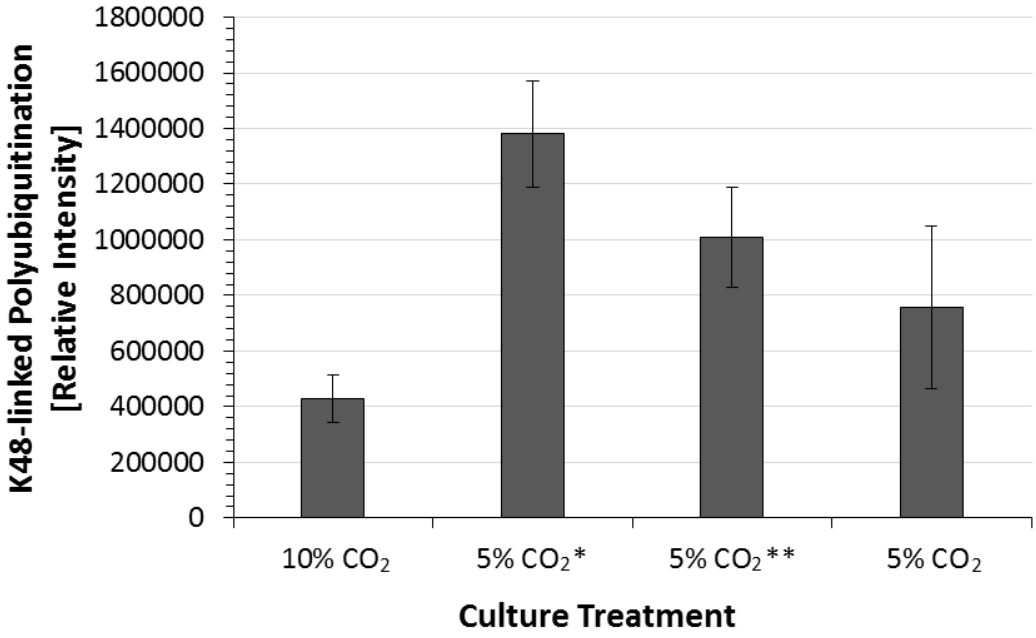


| Tukey's multiple comparisons test | Mean Diff. | 95.00% of CI of diff. | Sig.? | Adjusted P Value |
|---|---|---|---|---|
| 10% $CO_2$ vs. 5% $CO_2$* | -951432 | -1595293 to 307572 | Yes | 0.0064 |
| 10% $CO_2$ vs. 5% $CO_2$** | -578337 | -1222197 to 655323 | No | 0.0792 |
| 10% $CO_2$ vs. 5% $CO_2$ | -326456 | -970316 to 317404 | No | 0.4185 |
| 5% $CO_2$* vs. 5% $CO_2$** | -373095 | -270765 to 1016956 | No | 0.3172 |
| 5% $CO_2$* vs. 5% $CO_2$ | 624976 | -18884 to 1268836 | No | 0.0571 |
| 5% $CO_2$** vs. 5% $CO_2$ | 251881 | -391979 to 895741 | No | 0.6141 |

**Figure 3-2 Quantification of the effect of $CO_2$ on K48-linked polyubiquitination. Quantified and normalised data from Western blot replicates I-III (Figure 3-1). Relative Intensity is a calculated ratio between the K48-linked polyubiquitin signal and the vinculin loading control signal. * indicates extracellular pH control. ** indicates intracellular pH control. Error bars show standard deviation. n=3. Table below displays analysis of data using Tukey's post hoc comparison of data sets.**

be approximately equal, suggesting that this difference is not a result of unequal sample loading. Therefore, these findings are suggestive that $CO_2$ mediates the inhibition of K48-linked polyubiquitination.

However, drawing conclusions from raw Western blot data is largely inaccurate and unreliable; quantification of signal intensity and normalisation of data via loading controls ensures a more reliable analysis. Quantification of K48-linked ubiquitin and vinculin signal intensity via RawIntDensity enabled a more accurate understanding of the relationship between $CO_2$ and K48-linked polyubiquitination. The quantified and normalised data produced from Western blots I-III is shown in Figure 3-2. These findings indicate that $CO_2$ mediates the inhibition of K48-linked polyubiquitination.

A Shapiro-Wilke normality test indicated that all data sets were normally distributed. Data was therefore compared by one-way ANOVA with Tukey's post-hoc comparison of data sets. A one-way ANOVA confirmed that there is a significant difference in the extent of K48-linked polyubiquitination between the four treatments ($P < 0.005$). Comparison of data sets via Tukey's post-hoc analysis indicated that K48-linked polyubiquitination at 10% $CO_2$ is significantly different from at 5% $CO_2$ with extracellular pH control ($P < 0.05$). However, the difference in K48-linked polyubiquitination was demonstrated to be insignificant between 10% $CO_2$ and 5% $CO_2$ with intracellular pH control. Despite this, the data from this analysis is very close to significance ($P = 0.0792$), therefore further replicates may improve this experiment and demonstrate significance. It could be inferred that the reduction in K48-linked polyubiquitination observed at 10% $CO_2$ is mediated by the associated change in intracellular pH. However, K48-linked polyubiquitination at 5% $CO_2$ with intracellular pH control is not significantly different from 5% $CO_2$ ($P = 0.6141$), nor is it close to significance. On balance, it is highly likely that the effect observed on K48-linked polyubiquitination is mediated by $CO_2$ and not pH; however, further experiments will be required to demonstrate this formally. In future studies, utilisation of an ELISA assay would enable a more quantitative mechanism of assessment of K48-polyubiquitination, and would allow a large number of samples to be compared simultaneously.

It is interesting to note that the controls accounting for intracellular and extracellular pH elicited an unexpected effect; controlling for extracellular pH particularly induced a significant increase in K48-linked polyubiquitination. This result could be explained by the inhibitory effect observed on protein degradation by increasing pH (Fuller *et al*., 1989). Inhibition of protein degradation could, in turn, lead to an accumulation of K48-linked ubiquitin-conjugated proteins intended for degradation. Regardless, as both controls demonstrated an increase in K48-linked polyubiquitination, it is reasonable to conclude that the decrease in K48-linked polyubiquitination observed at 10% $CO_2$ is independent of the associated changes in pH.

The results of this investigation indicate that physiologically high concentrations of $CO_2$ mediate the inhibition of K48-linked polyubiquitination. These findings, therefore, provide supporting evidence for the hypothesis that the formation of carbamates observed on the ubiquitin K48 residue induce a change in the protein's function, and that increased carbamylation at the ubiquitin K48 residue inhibits the process of K48-linked polyubiquitination. This is likely a result of the change in electrostatic charge of K48's amine group, preventing the formation of an isopeptide bond with the C-terminal glycine residue of other ubiquitin monomers.

A limitation of these findings lies in the assumption that the inhibition of K48-linked polyubiquitination is a result of carbamate formation-induced inhibition of isopeptide bond formation. While this is a reasonable assumption to make, due to our limited understanding of carbamylation's effect on ubiquitin function, it is formally possible that $CO_2$ mediates this inhibition through an alternative mechanism.

## 3-3 Investigating the relationship between $CO_2$ and total protein per cell

Previous studies have highlighted the importance of K48-linked polyubiquitination in signalling for the select degradation of intracellular proteins via the 26S proteasome (Mallette and Richard, 2012). The findings presented in the above assay (section 3-2) demonstrate a $CO_2$-mediated inhibition of K48-linked polyubiquitination, independent of pH. Due to the demonstrated direct association between K48-linked polyubiquitination and protein degradation (Mallete and Richard, 2012), it was hypothesised that the observed $CO_2$-mediated inhibition of K48-linked polyubiquitination would, in turn, inhibit the degradation of proteins via the 26S proteasome. It was further hypothesised that this would induce an accumulation of proteins intended for degradation within the cell, eliciting an increase in total protein per cell.

### 3-3.1 Developing an assay to examine total protein per cell

An assay was developed in order to investigate the effect of $CO_2$ on total protein per live cell (section 2-4.3). HEK 293 cells were incubated at 5% $CO_2$ and 10% $CO_2$ for 18 h, ensuring full gassing of the cell culture. The number of live cells within a sample were quantified using 0.4% (w/v) Trypan Blue, a vital stain used to selectively colour dead/damaged cells blue. The remaining cell suspension was lysed via sonication, and the protein content of the whole cell lysates was measured via Bradford assay, using 5 µL of the lysate. Consideration of these values together enabled an approximation of the total protein per live cell. This approximation could then be compared between concentrations of $CO_2$ to investigate the effect of $CO_2$ on total protein per cell. A potential limitation of this assay lies in the use of a single cell type. It is possible that there is a degree of varying sensitivity to $CO_2$ between cell types, and thus a degree of variation in the effect of $CO_2$ on total protein per cell between cell types. For instance, pulmonary cells would be assumed to have a greater sensitivity to changes in $CO_2$ concentration. In future assays, utilisation of numerous cell types would provide insight into this possibility.

### 3-3.2 $CO_2$ elicits no effect on total protein per cell

Using the assay described (section 3-3.1), the effect of $CO_2$ on total protein per cell was examined. As shown in Figure 3-3, incubation at 10% $CO_2$ induced a small increase in total protein per cell, as well as total protein content in comparison to incubation at 5% $CO_2$. However, a *t*-test demonstrated that this difference was not significant in either case ($P > 0.05$). This finding is not supportive of the stated hypothesis and contradicts the outcomes inferred from the K48-linked polyubiquitination assay (section 3-2). Conversely, the data here indicates that $CO_2$ elicits no effect on total protein per cell.

These observations may be unsurprising when the whole scope of $CO_2$-mediated physiological effects are considered; $CO_2$ has been implicated in a number of biological processes, such as metabolism. Moreover, metabolism has been demonstrated to elicit effects on proteolysis and degradation of all cell proteins (Goldberg and St. John, 1976). As a result, it is possible that due to the effect of $CO_2$ on many cellular processes, and the effect these processes have on protein turnover, the relationship between $CO_2$ and K48-linked polyubiquitination-dependent protein degradation are unobservable when

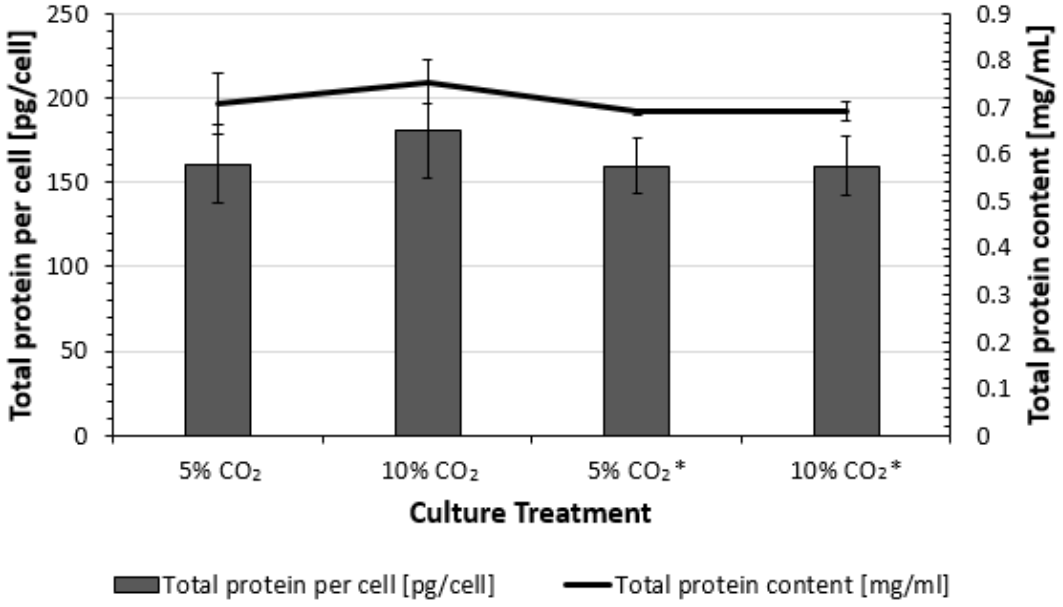


**Figure 3-3 The effect of $CO_2$ on total protein per cell and total protein content. Total protein per cell calculated from number of live cells within a sample and total sample protein content. * indicates 20 µg/mL CHX treatment. Error bars show standard deviation. n=3.**

using this assay. Alternatively, it is important to note that protein degradation is not regulated exclusively by the ubiquitin-proteasome system: the findings presented in this assay may be affected by artefacts produced by lysosome-mediated protein degradation, for example (Dunn, 1994).

The methodology of this assay is complicated by a number of limitations, which may have had an adverse effect on the clarity of the results produced, compared to those initially predicted. Firstly, the method of quantifying total protein per cell may have incited errors due to the inherent inaccuracies in the techniques used. The number of cells within a sample was calculated using a haemocytometer. While this method is effective for quickly estimating the population of cells within a sample, cytometry might offer a more robust methodology. The significant degree of variation in values when determining cell populations using a haemocytometer has been attributed to cellular movement within the sample, observer inaccuracy and uneven distribution of cells (Freund and Carol, 1964; Gadeholt, 2009). In subsequent assays, therefore, an automated cell counter could be used in order to remove such inaccuracies in the number of cells counted within a sample (Salinas *et al*., 1997). Similarly, the method used to calculate the protein content of a sample has an inherent inaccuracy: calculating the concentration of a protein sample via Bradford assay is a useful tool for estimating protein concentration and can be done on numerous samples simultaneously. However, it is subject to a number of external variables such as temperature and pipetting error, thus limiting the accuracy of any measurement taken. As a result of these limitations, the value obtained for total protein per cell is subject to potential error and variation. Moreover, aside from these limitations which are intrinsic to the techniques utilised in this project, artefacts in the data may have been produced as a result of additional exogenous factors affecting protein turnover. Removing the potential for other variables to influence total protein per cell would enable a better understanding of the effect had by $CO_2$.

The ongoing synthesis of new proteins presents perhaps the most significant of these variables. Therefore, the effect of $CO_2$ on total protein per cell was examined while blocking the synthesis of new proteins. It was hypothesised that controlling for the input of new proteins would enable a better

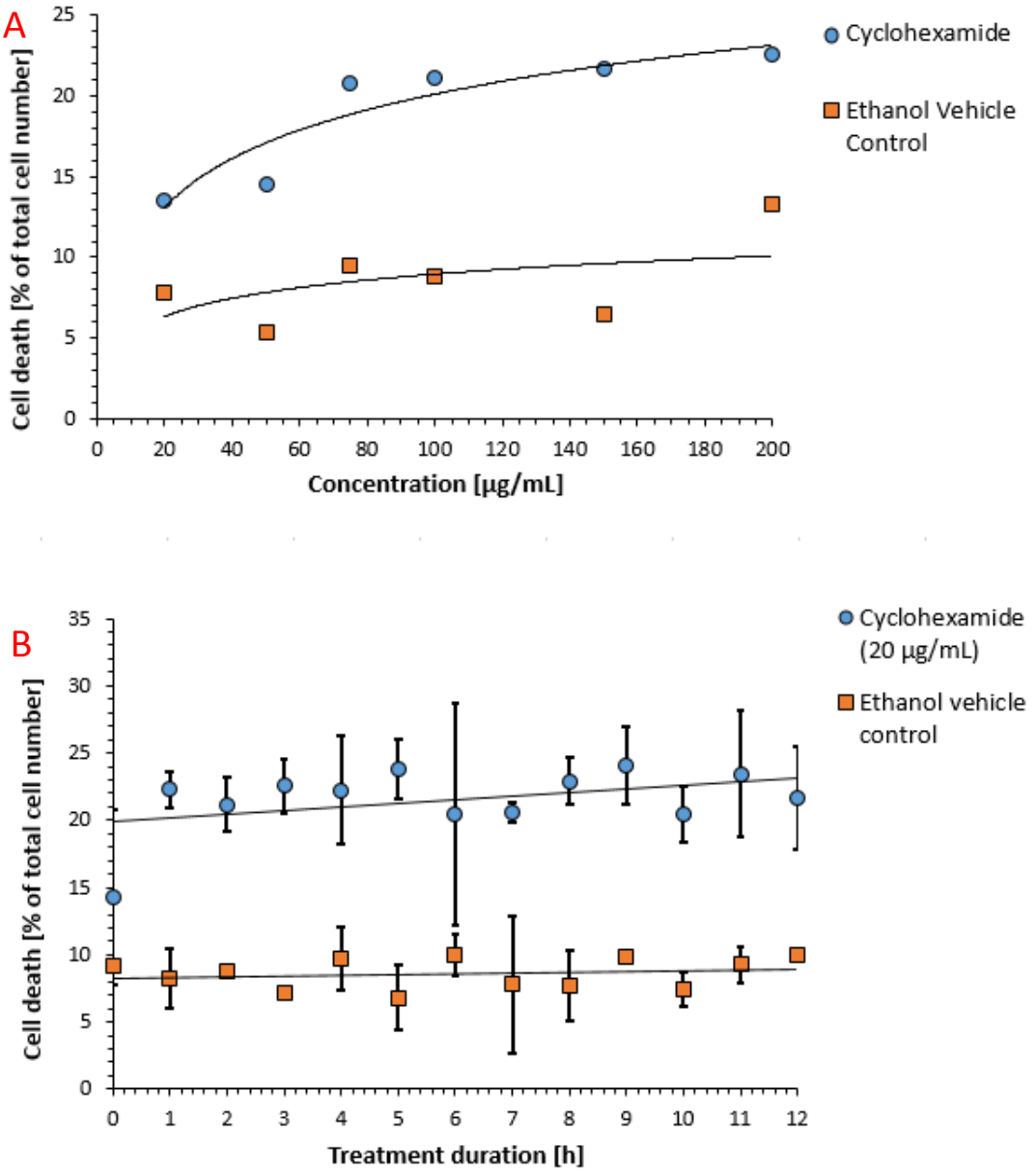


**Figure 3-4 Measuring CHX toxicity. A: Dose-response assay measuring the effect of CHX concentration on cell viability. B: Time-scale assay measuring the effect of duration of CHX treatment (20 µg/mL) on cell viability. Ethanol vehicle control ensures observations are a result of the effect of CHX. Error bars show standard deviation. (B) n=3**

understanding of how $CO_2$ mediates total protein per cell. The synthesis of new proteins was blocked via treatment with 20 µg/mL CHX for 18 h, a common method for the inhibition of protein synthesis in mammalian cells (Siegal and Sisler, 1996).

The chosen concentration of CHX treatment was determined via findings produced from toxicity assays (section 2-4.1). An ethanol vehicle-treated control ensured that the effect on cell viability was a result of CHX treatment. This enabled the maximum inhibition on protein synthesis to be achieved while simultaneously limiting the effect had on cell viability. Figure 3-4 (A) shows the effect of increasing CHX concentration on cell viability. Due to the relatively low induction of cell death/damage, 20 µg/mL CHX was selected for a time-course assay. As shown in Figure 3-4 (B), examining the effect of treatment duration of 20 µg/mL CHX on cell viability demonstrated that duration of treatment elicited no significant effect on cell viability. From these findings, it was deduced that treatment of 20 µg/mL CHX would provide an appropriate treatment for the inhibition of protein synthesis in mammalian cells without compromising cell viability.

As shown in Figure 3-3, the effect of $CO_2$ had no effect on total protein per cell, as well as total protein content, even when blocking the synthesis of new proteins. This was confirmed using a *t*-test, demonstrating that the difference in total protein per cell as well as total protein content between 5% $CO_2$ and 10% $CO_2$ is not significant in both cases ($P > 0.05$).

The results of this investigation indicate that $CO_2$ does not elicit an effect on total protein per cell. As discussed, this is potentially a result of the gross effect of $CO_2$ on biological processes, with consequent implications on total protein turnover. Despite the findings presented in this assay, there is insufficient evidence to conclude that $CO_2$ categorically does not elicit an effect on total protein per cell; it is possible that inhibition of degradation, and accumulation within the cell, occurs at the level of individual proteins, as opposed to the entire cellular proteome. A limitation of this investigation lies in the relatively gross experimental approach: utilisation of more sensitive methods, which enable the examination of rapid protein turnover via the ubiquitin-proteasome system, are required for future insight into this possibility.

## 3-4 Conclusion

This chapter has discussed the development of an assay used to examine the relationship between $CO_2$ and K48-linked polyubiquitination. It was hypothesised that a $CO_2$-mediated increase in carbamate formation on the K48 residue of ubiquitin would inhibit the process of polyubiquitination at this residue. The results of this assay presented evidence supporting this hypothesis as a reduction in K48-linked polyubiquitination was observed at 10% $CO_2$ in comparison to 5% $CO_2$, independent of pH. Parallel to this investigation, the relationship between $CO_2$ and total protein per live cell was examined. It was hypothesised that a $CO_2$-mediated inhibition of K48-linked polyubiquitination would, in turn, elicit an effect on functions regulated by this process; specifically, the selective degradation of intracellular proteins. It was further hypothesised that a $CO_2$-mediated inhibition of K48-linked polyubiquitination-dependent protein degradation would induce an accumulation of proteins intended for degradation within the cell, ultimately resulting in an increase in total protein per cell. Contrary to expectations, it was observed that $CO_2$ elicited no effect on total protein per cell. In regard to these findings, it was hypothesised that the $CO_2$-mediated inhibition of protein degradation may only be observed at the level of individual proteins, particularly those known to be directly degraded in a K48-linked polyubiquitination-dependent manner.

# Chapter 4: $CO_2$ and the NF-κB signalling pathway

## 4-1 Overview

Drawing from the conclusions reached in the previous chapter, it was hypothesised that, despite a lack of evidence supporting the $CO_2$-mediated regulation of total protein per cell, $CO_2$ may elicit an impact on the degradation of proteins at an individual level. In addition, it was further hypothesised that proteins degraded as a direct result of K48-linked polyubiquitination form the most likely candidates for this effect, in which case cells would exhibit an accumulation of these proteins under conditions of physiologically high concentrations of $CO_2$.

The significance of K48-linked polyubiquitination has, moreover, been implicated in the activation of the canonical NF-κB signalling pathway via signalling for the selective degradation of IκB (Mathes *et al*., 2012; Ohtake *et al*., 2016). IκB forms direct interactions with NF-κB dimers, masking their NLS and inhibiting their translocation to the nucleus (Chen and Ghosh, 1999). Stimulation-dependent phosphorylation of IκB marks the NF-κB inhibitor for degradation via the ubiquitin-proteasome pathway (Alkalay *et al*., 1995). Liberation of NF-κB dimers from IκB exposes their NLS, enabling the dimers to translocate to the nucleus and induce expression of target genes (Hoesel and Schmid, 2013).

Inhibition of K48-linked polyubiquitination was previously shown to be likely mediated in a $CO_2$ controlled manner. As the activation of canonical NF-κB signalling is known to be regulated by the K48-linked polyubiquitination-dependent degradation of IκB, it was hypothesised that $CO_2$ may mediate the degradation of IκB. It was further anticipated that under conditions of physiologically high levels of $CO_2$, the inhibited degradation of IκB would result in its subsequent accumulation within the cell. Moreover, this inhibition of IκB degradation would prompt the sequestration of NF-κB dimers within the cytoplasm, preventing the induction of target genes in the nucleus. As a result, it was expected that under physiologically high concentrations of $CO_2$, an inhibition of NF-κB signalling would be observed.

The results discussed throughout this chapter are therefore based on investigations into the $CO_2$-mediated effect on NF-κB signalling. Utilisation of a transcriptional reporter cell line enabled quantification of NF-κB activation and provided insight into the effect of physiologically high $CO_2$ concentrations. Parallel to this investigation, examining the effect of $CO_2$ on the degradation of IκBα aided in elucidating the relationship between $CO_2$ and K48-linked polyubiquitination-dependent canonical activation of NF-κB signalling.

## 4-2 Investigating the relationship between $CO_2$ and NF-κB signalling

Based on our understanding of K48-linked polyubiquitination-dependent canonical activation of NF-κB signalling, alongside findings which indicated a likely $CO_2$-mediated inhibition of K48-linked polyubiquitination, it was hypothesised that an inhibition of NF-κB signalling would be observed at physiologically high concentrations of $CO_2$, in concordance with existing reports (Cummins *et al*., 2010; Keogh *et al*., 2017; O'Toole *et al*., 2009).

### 4-2.1 Developing an assay to investigate NF-κB signalling

In order to test the above hypotheses, an assay was developed to examine the effect of $CO_2$ on the dose-dependent activation of NF-κB signalling (section 2-4.5). Transcriptional reporter cell lines NF-κB/293/GFP-Luc and NF-κB/U251/GFP-Luc were employed for quantification of NF-κB signalling via GFP fluorescence intensity, in turn functioning as a reporter of NF-κB gene expression. Tumour necrosis factor (TNF)-α, a primary cytokine implicated in a multitude of vital processes, including canonical activation of NF-κB, was utilised to activate the NF-κB signalling pathway (Horiuchi *et al*., 2010; Osborn *et al*., 1989). A dose-response assay of NF-κB signalling to TNF-α (2 ng/mL to 100 ng/mL) was conducted at both 5% $CO_2$ to 10% $CO_2$ for 18 h, enabling the effect of $CO_2$ to be observed on NF-κB signalling activation. Following this incubation period, cells were aspirated and lysed in 300 µL 1x lysis buffer. A sample of the cell lysate was analysed to quantify the fluorescence intensity of the GFP. This was achieved through excitation/emission of light with wavelengths 485/530 nm. A portion of the remaining cell lysate was analysed by Bradford assay to provide a value for total protein content within the sample. Using these two measurements, a value of fluorescent counts per µg of protein could be calculated and compared, enabling the relationship between $CO_2$ and NF-κB signalling to be examined.

### 4-2.2 $CO_2$-mediated suppression of NF-κB signalling

The above assay was used to investigate the proposed hypothesis. NF-κB/293/GFP-Luc cells were treated with an increasing dosage of TNF-α and

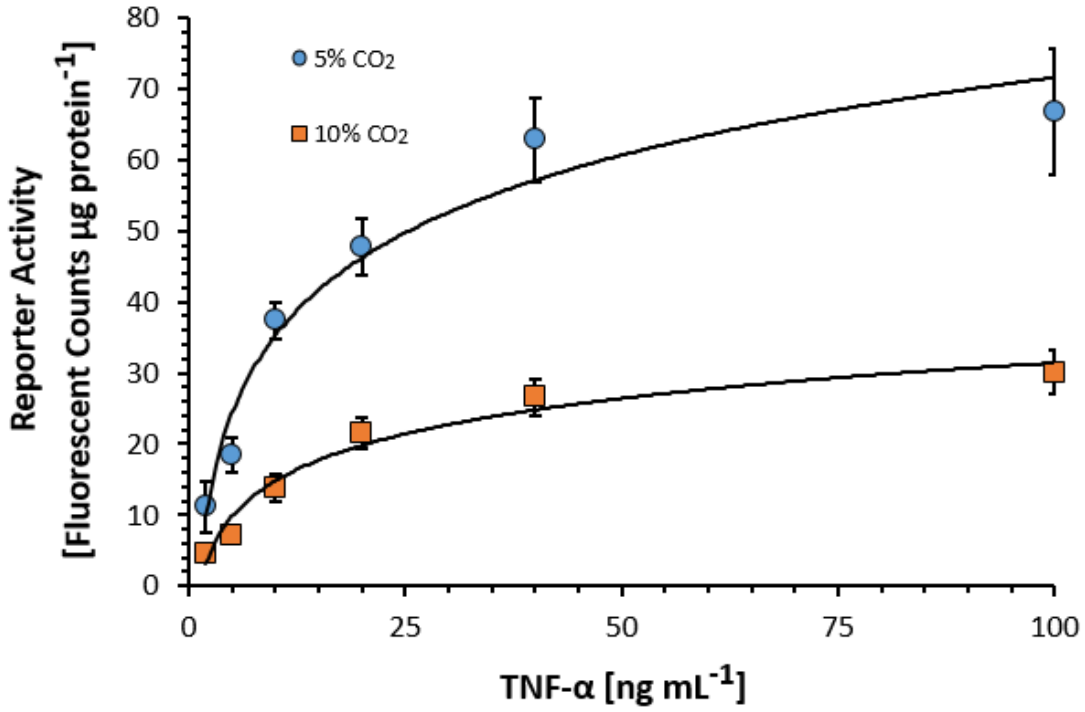


**Figure 4-1 The effect of $CO_2$ on NF-κB signalling. Dose-response of NF-κB signalling to increasing concentrations of TNF-α at 5% $CO_2$ and 10% $CO_2$. Data points shown are fluorescent counts per µg protein. Error bars show standard deviation. n=3.**

incubated at 5% $CO_2$ and 10% $CO_2$ respectively for 18 h. The quantification of NF-κB signalling is shown in Figure 4-1.

The results displayed in Figure 4-1 demonstrate that NF-κB reporter activity increases with increasing concentrations of TNF-α. From the dose-response curves produced, a substantial difference in reporter activity can be observed between 5% $CO_2$ and 10% $CO_2$; in comparison to incubation at 5% $CO_2$, incubation at 10% $CO_2$ induces inhibition of NF-κB signalling in cells at all concentrations of TNF-α (2 ng/mL to 100 ng/mL). Furthermore, a *t*-test confirmed that the difference in reporter activity between 5% $CO_2$ and 10% $CO_2$ at 100 ng/mL TNF-α was statistically significant ($P < 0.001$). The findings produced by this assay recapitulate the findings of previous work, demonstrating a $CO_2$-mediated regulation of NF-κB signalling (Cummins *et al*., 2010; Keogh *et al*., 2017; O'Toole *et al*., 2009). Additionally, this work provided a model cell system that could be used to dissect the molecular components that contribute to this inhibitory effect.

The findings concluded from this assay are potentially limited by the delay in the effect of $CO_2$ in comparison to TNF-α. While the effect had on the cells by TNF-α is likely near-instantaneous, the effect had by $CO_2$ is dependent on the diffusion of the gas into the medium and thus the cells, and likely takes significantly longer. This may result in the activation of NF-κB prior to the inhibition proposed to be had by increased concentrations of $CO_2$. To account for this in future assays, pre-conditioning of cell culture with $CO_2$ prior to the addition of TNF-α would minimise this possibility, and enable a greater insight into the effect had by $CO_2$ on NF-κB signalling.

### 4-2.3 Investigating the involvement of ubiquitin lysine residues in the $CO_2$-mediated suppression of NF-κB signalling

The results illustrated in Figure 4-1 provide compelling evidence in support of the proposed hypothesis, in demonstrating the $CO_2$-mediated suppression of NF-κB signalling. However, these findings alone are of limited consequence as they provide no insight into how the observed suppression is achieved. One hypothesis of this thesis states that the $CO_2$-mediated suppression of NF-κB signalling is a result of the $CO_2$-mediated modification of ubiquitin function, in particular via the inhibition of K48-linked polyubiquitination-dependent degradation of IκB. In order to provide greater insight into how the observed suppression of NF-κB signalling is mediated, the involvement of ubiquitin's lysine residues was explored.

The respective roles played by ubiquitin's lysine residues in the $CO_2$-mediated suppression of NF-κB signalling were investigated using the above assay; NF-κB/293/GFP-Luc transcriptional reporter cells were transfected with wild-type (WT) ubiquitin and knockout (KO) ubiquitin, in which K6, K11, K27, K29, K33, K48 and K63 are substituted for inert arginine residues. In addition, ubiquitin mutants wherein all but one of the aforementioned lysine residues were replaced by an arginine residue (K48, K33 and K63) were transfected. This therefore provided a platform from which to investigate the involvement of specific ubiquitin lysine residues of interest in the $CO_2$-mediated suppression of NF-κB signalling. The transfection of cells with WT ubiquitin functioned as a

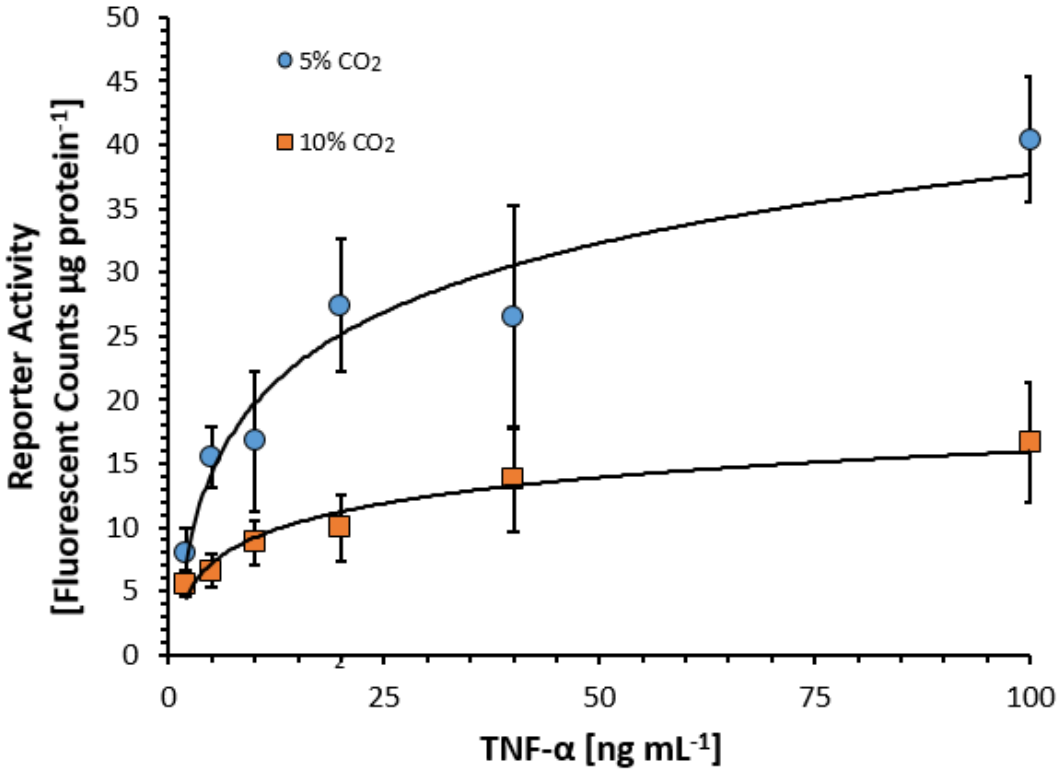


**Figure 4-2 The effect of WT ubiquitin overexpression on the $CO_2$-mediated suppression of NF-κB signalling. Dose-response of NF-κB signalling to increasing concentrations of TNF-α at 5% $CO_2$ and 10% $CO_2$. Data points shown are fluorescent counts per µg protein. Error bars show standard deviation. n=3.**

vital control to ensure that any changes observed were a result of lysine mutations and not caused by effects associated with the transfection protocol, such as cellular toxicity or the levels of ubiquitin present in transfected compared to non-transfected cells. In future studies, a vector-only control should be employed to ensure that any observed effects were not due to the plasmid vector.

Figure 4-2 demonstrates that transfecting NF-κB/293/GFP-Luc cells with WT ubiquitin induces no significant effect on the dose-response of NF-κB signalling to TNF-α. The cells display a slight reduction in reporter activity at both 5% $CO_2$ and 10% $CO_2$; however, a *t*-test demonstrated that the difference in reporter activity between 5% $CO_2$ and 10% $CO_2$ at 100 ng/mL TNF-α was statistically significant ($P < 0.05$). Furthermore, an extra sum of squares *F*-test demonstrated that no one curve can explain the data sets at 5% $CO_2$ and 10% $CO_2$; the curves are therefore different. The overall reduction in reporter activity

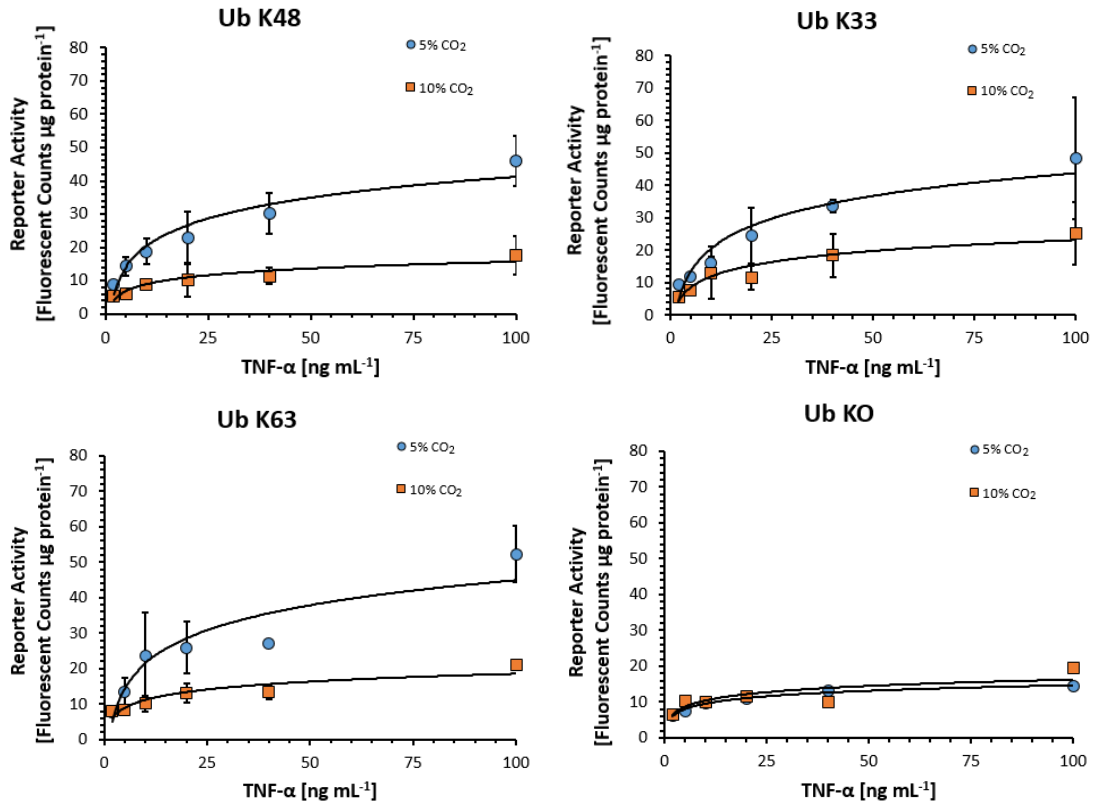


**Figure 4-3 The effect of overexpressing ubiquitin mutants K48, K33, K63 and KO on the $CO_2$-mediated inhibition of NF-κB signalling. Dose-response of NF-κB signalling to increasing concentrations of TNF-α at 5% $CO_2$ and 10% $CO_2$. Data points shown are fluorescent counts per µg protein. Error bars show standard deviation. Ub K48 n=3, Ub K33 n=2, Ub K63 n=2, Ub KO n=1. n represents number of biological replicates.**

at both 5% $CO_2$ and 10% $CO_2$ is possibly a by-product of the transfection protocol: as discussed, transfection-induced cellular toxicity may effect NF-κB signalling.

As shown in Figure 4-3, the overexpression of ubiquitin mutants K48, K33 and K63 has no significant effect on the $CO_2$-mediated inhibition of NF-κB signalling, and provides little insight into the roles played by these particular lysine residues. Interestingly, overexpression of the ubiquitin KO mutant induces minimal activation of NF-κB signalling. This was hypothesised to be a downstream consequence of the inhibition of polyubiquitination; the ubiquitin KO mutant cannot function as a receiver for E2-conjugating enzyme-bound ubiquitin, in turn resulting in complete failure of NF-κB activation with no observable response to elevated concentrations of $CO_2$. Ultimately, the findings gleaned from this assay provide very little insight into the roles played by individual ubiquitin lysine residues in the $CO_2$-mediated inhibition of NF-κB

signalling. This may be a result of the small sample size; additional replicates are thus required to further elucidate this possibility. In future studies, simultaneous transfection of ubiquitin mutants would provide greater reliability in the findings produced due to the use of the same controls. However, this would provide a significant amount of work and would likely prove difficult from a practicality standpoint. Alternatively, it was posited that the utilisation of these mutants had too great an impact on the cellular system; knockout of six lysine residues likely perturbs a number of ubiquitin-regulated processes, resulting in the production of artefacts within this assay. It was subsequently hypothesised that the use of ubiquitin mutants where all but one lysine are intact would facilitate the proper function of ubiquitin for other processes in the cell. Accordingly, it was anticipated that utilisation of these mutants would enable the role of the lysine residue of interest in the $CO_2$-mediated inhibition of NF-κB signalling to be better examined.

### 4-2.4 K48R-mediated suppression of NF-κB signalling

The overarching hypothesis of this thesis states that the $CO_2$-mediated suppression of NF-κB signalling occurs as a result of inhibited K48-linked polyubiquitination-dependent degradation of IκB; the involvement of ubiquitin's K48 residue in NF-κB signalling was therefore examined. In addition, it was further suggested that inhibiting the function of the ubiquitin K48 residue would induce a suppression in NF-κB signalling similar to that observed at 10% $CO_2$, in turn, mimicking the inhibitory effect hypothesised to be had by carbamylation at this site.

The role played by ubiquitin's K48 residue in the $CO_2$-mediated suppression of NF-κB signalling was investigated by implementing the above assay; in addition, NF-κB/293/GFP-Luc transcriptional reporter cells were transfected with a lysine 48 to arginine (K48R) ubiquitin mutant. In this mutant, the functional lysine residue is replaced by an inert arginine residue, which is unlikely to mediate any direct effect on the functional properties of ubiquitin. Removal of the lysine at this position, however, inhibits the formation of a carbamate. This construct therefore provided a platform from which to investigate the involvement of the K48 residue of ubiquitin in $CO_2$-mediated

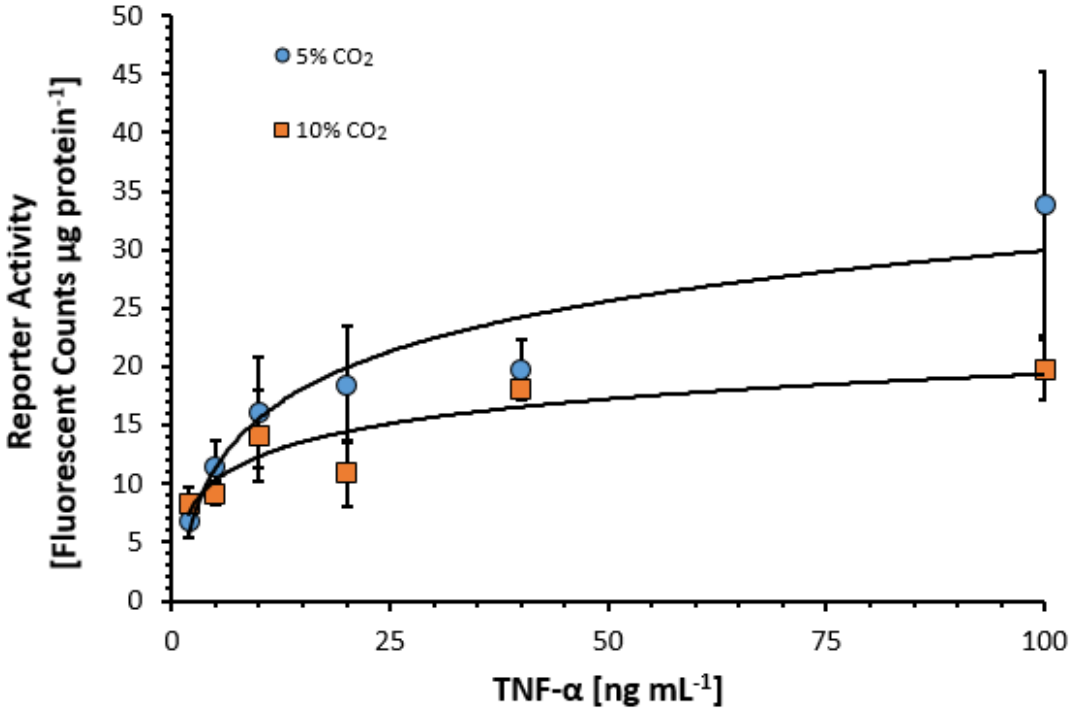


**Figure 4-4 The effect of ubiquitin mutant K48R overexpression on the $CO_2$-mediated suppression of NF-κB signalling. Dose-response of NF-κB signalling to increasing concentrations of TNF-α at 5% $CO_2$ and 10% $CO_2$. Data points shown are fluorescent counts per µg protein. Error bars show standard deviation. n=2.**

suppression of NF-κB signalling, and enabled the importance of carbamylation in this process to be more directly assessed.

Transfecting NF-κB/293/GFP-Luc cells with K48R ubiquitin induces a significant impact on the dose-response of NF-κB signalling to TNF-α, in a $CO_2$-dependent manner. It can be observed from Figure 4-4 that overexpression of the K48R mutant results in the inhibition of the NF-κB dose-response to TNF-α, in turn, mimicking the effect of $CO_2$-mediated inhibition. A *t*-test was used to confirm that the difference in reporter activity between 5% $CO_2$ and 10% $CO_2$ was not statistically significant for all TNF-α concentrations ($P > 0.05$). Moreover, an extra sum of squares *F*-test demonstrated that one curve can explain the data sets at both 5% $CO_2$ and 10% $CO_2$. The curves are therefore statistically indistinguishable. The observed effect is likely facilitated by the dominant negative effect had by the K48R mutant; this mutation both inhibits K48-linked polyubiquitin chain formation on IκB and prevents the formation of carbamates at this site, therefore reducing the influence of $CO_2$ on NF-κB signalling.

The results of this assay indicate that the functionality of the ubiquitin K48 residue plays an important role in the activation of NF-κB signalling, supportive of previous findings (Ohtake *et al*., 2016). A lysine to arginine mutation at this residue results in the inhibition of NF-κB signalling, similar to that mediated by increased levels of $CO_2$. This therefore suggests that the suppression of NF-κB signalling mediated by $CO_2$ is achieved via the $CO_2$-dependent modification of the ubiquitin K48 residue, most likely through the formation of a carbamate at this site. It is possible that the carbamylation of this residue induces a conformational change or, alternatively, physically blocks the site for ubiquitin conjugation, in both cases resulting in the inhibition of K48-linked polyubiquitin chain formation on IκB, similar to the hypothesised effect of the K48R mutant. Moreover, preceding findings from this thesis implicated K48 carbamylation in a reduction in K48-linked polyubiquitination. It was hypothesised that this would, in turn, result in the inhibition of the selective degradation of IκB and the canonical activation of NF-κB signalling.

### 4-2.5 Further examination of the involvement of ubiquitin lysine residues in the $CO_2$-mediated suppression of NF-κB signalling

The above assays were focused primarily on the involvement and functionality of the ubiquitin K48 residue in the $CO_2$-mediated inhibition of NF-κB signalling. These assays provided supporting evidence for the overarching hypothesis, and have implied that increased carbamylation at the ubiquitin K48 residue ultimately elicits the inhibition of NF-κB signalling.

However, it is formally possible that $CO_2$ may have an effect at sites other than K48, and that carbamylation of ubiquitin's six other lysine residues may elicit similar outcomes. In order to validate these findings, the roles of ubiquitin's six other lysine residues in the $CO_2$-mediated suppression of NF-κB signalling must be elucidated. To achieve this, the effects of overexpressing ubiquitin lysine to arginine mutants for each of the additional residues on the NF-κB dose-response to TNF-α must be observed at 5% $CO_2$ and 10% $CO_2$.

### 4-2.6 Issues with cell lines

Whilst investigating the roles of ubiquitin's six other lysine residues in the $CO_2$-mediated inhibition of NF-κB signalling, issues arose regarding the reporter cell line in use, which prevented the collation of further reliable data. This ultimately precluded the substantiation of any conclusions regarding the contributions of ubiquitin's six other lysine residues. In this section, the issues encountered, as well as potential alternative routes for future investigations, will be discussed.

The NF-κB/293/GFP-Luc transcriptional reporter cell line previously employed for the generation of data (Figure 4-1, Figure 4-2, Figure 4-3 and Figure 4-4) began to produce inconsistent and irreproducible data. As shown in Figure 4-5, the inhibitory effect previously observed by 10% $CO_2$ in comparison to 5% $CO_2$ on NF-κB signalling appeared to diminish. Additionally, the induction of NF-κB signalling activation by TNF-α appeared to become inhibited; a 50 fold

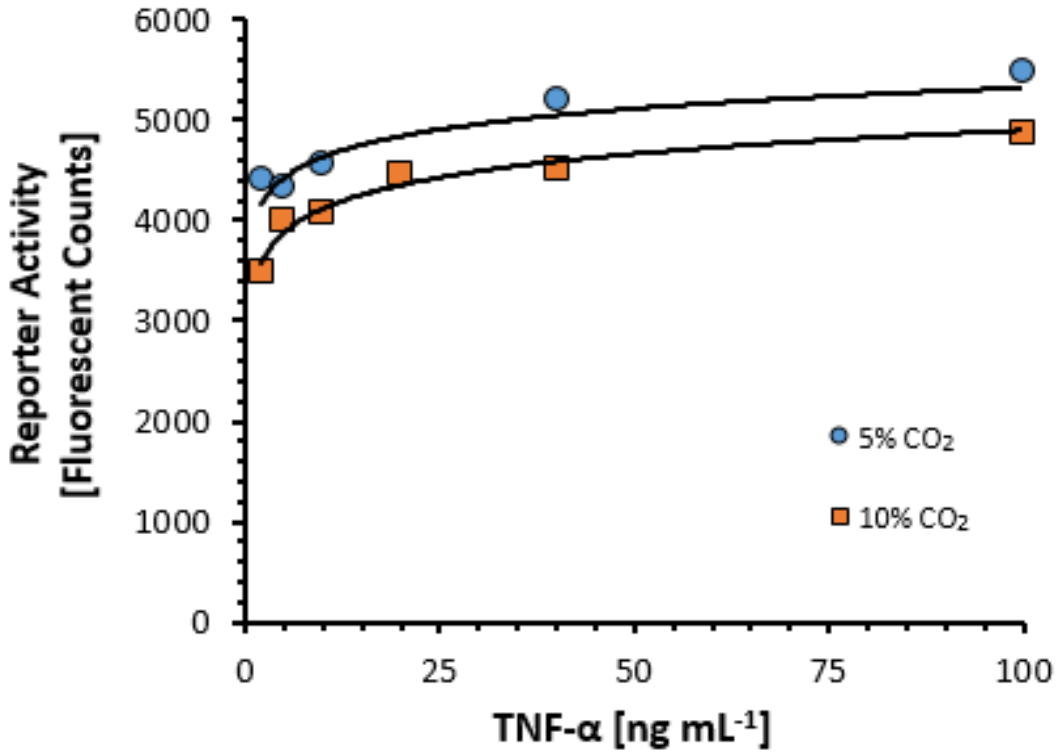


**Figure 4-5 NF-κB/293/GFP-Luc transcriptional reporter cell line issues. NF-κB dose-response to TNF-α at 5% $CO_2$ and 10% $CO_2$ demonstrates an inhibited response to TNF-α alongside a reduction in $CO_2$-mediated inhibition.**

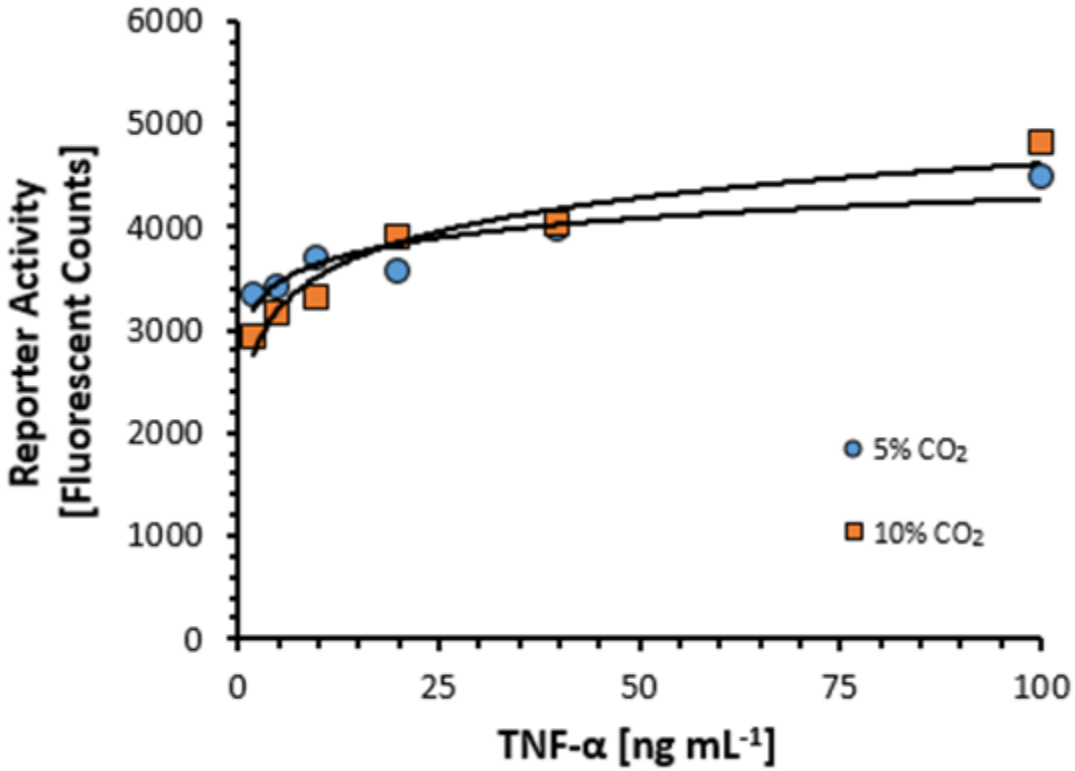


**Figure 4-6 NF-κB/U251/GFP-Luc transcriptional reporter cell line issues. NF-κB dose-response to TNF-α at 5% $CO_2$ and 10% $CO_2$ demonstrates an inhibited response to TNF-α alongside a reduction in $CO_2$-mediated inhibition.**

increase in TNF-α concentration (from 2 ng/mL to 100 ng/mL) induced a comparatively small increase in reporter activity and appeared to have very little effect on the induction of the signalling pathway. Furthermore, a significant reduction in peak fluorescent counts was observed, indicating a reduction in the activity of the reporter. The peak fluorescent count value displayed in Figure 4-5 equates to 5484 counts. In comparison, prior to the encountered issues regarding cell line, the NF-κB/293/GFP-Luc transcriptional reporter cell line would generate a peak fluorescent count value of approximately 45,000.

The observations made could be explained by issues with the reporter cell line or by issues intrinsic to the assay. To investigate this possibility formally, an ELISA assay could be conducted against the cytokine interleukin-8, a known inducer of NF-κB signalling (Manna and Ramesh, 2004). Interleukin-8 would likely be inhibited by $CO_2$ regardless of whether the reporter cell line is functioning as intended. In turn, this would provide insight as to whether the observations made are a result of issues with the reporter, issues intrinsic to the assay or due to damage in the cell's response mechanism to $CO_2$.

A new, as yet unused batch of TNF-α was employed to account for the potential inactivation of the prior batch as a result of subjection to excessive freeze-thaw cycles; however, this had no impact on reporter activity. Subsequently, due to the observed reduction in the $CO_2$-mediated inhibition of NF-κB signalling, it was hypothesised that inaccurate control of $CO_2$ in the incubators may have been responsible for this artefact. Utilisation of a handheld $CO_2$ monitor would have confirmed the accuracy of the incubator's $CO_2$ concentration, however, this piece of equipment was not available for use in this project. Alternatively, measuring the pH of medium post-incubation would have provided an approximate estimation of the incubator's $CO_2$ concentration. Despite this, the use of new incubators had no impact on the reporter activity. Ultimately, as a result of the low fluorescence values produced, it was assumed that the issue at fault lay within the reporter cell line. It is feasible that the GFP reporter construct within the cell line had become mutated over the high number of cell passages to which it was subjected, with downstream effects on the functionality of the reporter. This is a fairly reasonable assumption due to the lack of utilisation of selection markers on the cell line. Following from this reasoning, an alternative reporter cell line, U251, was implemented into the pre-existing TNF-α dose-response assay. The cells selected contained the same NF-κB/GFP-Luc transcriptional reporter as in previous assays. However, use of this cell line also generated unforeseen issues. As shown in Figure 4-6, this cell line also exhibited significantly low fluorescent counts, and no significant difference between the activity of NF-κB signalling at 5% $CO_2$ and 10% $CO_2$ was observed. As this cell line was only recently acquired, it was extremely unlikely that the GFP reporter had been mutated within the cell line.

A number of strategies could be explored to identify errors within the assays; however, due to time constraints they were not identified during the course of this project. GFP in the U251 reporter cell line had a short half-life, and was in an unstable form to reduce accumulation and toxicity in mammalian cells (Dr Darius Widera, University of Reading, personal communication). However, unstable GFP is not a suitable method for quantification and is generally used as a control for verification of activity, as opposed to quantification of activity

at late end points. In order to optimise this assay, it would be beneficial to measure the reporter activity through the luciferase of the promoter cell line as opposed to GFP, as this would provide a far more accurate, reliable and quantifiable value. Alternatively, a replacement of the original HEK 293 reporter cell line would enable insight into the hypothesis that the loss of responsiveness to TNF-α observed was a result of the loss of reporter construct from the cell line. Moreover, other external factors surrounding the assay may be responsible for the errors encountered; further exploration of these factors may yield cheaper alternatives to the purchase of a new cell line. For example, the use of serum-free media could easily account for and rectify the potential adverse effects that TNF-α pre-existent in the media used in these assays may have had on the activity of the NF-κB signalling pathway.

## 4-3 Investigating the relationship between $CO_2$ and IκB degradation

The above assays demonstrated the $CO_2$-mediated inhibition of NF-κB signalling. Moreover, overexpression of a mutant ubiquitin K48R residue resulted in the inhibition of NF-κB signalling, mimicking the suppression mediated by $CO_2$. These findings inferred that the $CO_2$-mediated inhibition of NF-κB signalling is a result of a modification in the function of the K48 ubiquitin residue. Moreover, earlier assays demonstrated a likely $CO_2$-mediated inhibition of K48-linked polyubiquitination, with potential downstream consequences on the selective degradation of particular proteins. Taken together, it was posited that the $CO_2$-linked inhibition of NF-κB signalling is a result of a decreased ability of cells to undergo K48-linked polyubiquitin-dependent degradation of the IκB inhibitory proteins. A decrease in IκB degradation would, in turn, induce an increase in sequestration of NF-κB dimers within the cytoplasm, inhibiting their translocation into the nucleus and the associated expression of target genes. To examine this possibility, the effect of $CO_2$ on the degradation of IκB was observed. It was hypothesised that $CO_2$ would mediate the inhibition of IκB degradation, in turn resulting in an inhibition of NF-κB signalling via the canonical activation pathway. In this section, the effect of $CO_2$ on the degradation of IκBα, a member of the inhibitory protein family, is examined.

### 4-3.1 Developing an assay to investigate IκBα degradation

In order to investigate the relationship between $CO_2$ and IκBα degradation, an assay was developed (section 2-4.6). The induction of the canonical NF-κB signalling pathway, and the consequent degradation of IκBα was achieved through treatment of HEK 293 cells with 100 ng/mL TNF-α. While alternative mechanisms of NF-κB activation exist, such as those regulated by LPS and interleukin-1β, TNF-α induced canonical activation of NF-κB signalling occurs via the tumor necrosis factor receptor (TNFR) family. Upon binding of TNF-α, TNFR1 recruits the adaptor protein TRADD, which in turn recruits the TNFR-associated factor (TRAF) 2. A signalling cascade following the recruitment of TRAF2 ultimately induces the activation of IKK, resulting in the degradation of

IκBα, and activation of NF-κB signalling (Napetschnig *et al*., 2013). 100 ng/mL TNF-α was selected to maximise the potency of TNF-α, and induce the greatest degree of IκBα degradation possible. In turn, this would enable the effect elicited by $CO_2$ to be determined more easily. Consequently, cells were incubated at 5% $CO_2$ and 10% $CO_2$ respectively for 3 h, with no pre-conditioning. This short timeframe was selected to reduce the possibility of IκBα regenerating prior to measuring the extent of its degradation. Controls accounting for the intracellular and extracellular pH changes associated with the shift from 5% $CO_2$ to 10% $CO_2$ ensured that observed changes in IκBα degradation were directly a result of the change in $CO_2$ concentration. Cells were lysed via sonication and the resultant lysates separated via a 12% SDS-PAGE gel. Due to IκBα's relatively small mass of 36 kDa, the use of a 12% SDS-PAGE gel ensured that it did not migrate too far through the SDS-PAGE gel. Samples were electroblotted onto a nitrocellulose membrane and the extent of IκBα present was assayed by Western blot, probed using an anti-IκBα antibody. To prevent the occurrence of experimental artefacts produced by unequal sample loading, a vinculin loading control was used. Calculating the relative intensity of the IκBα sample against the vinculin loading control produced a more reliable final assessment of the effect of $CO_2$ on IκBα degradation.

### 4-3.2 $CO_2$-mediated inhibition of IκBα degradation

The results of the above assay are presented in Figure 4-7. From this data, it can be observed that incubation at 10% $CO_2$ mediates an inhibited degradation of IκBα in comparison to incubation at 5% $CO_2$ (with controls for intracellular and extracellular pH). Unexpectedly, 5% $CO_2$ without a pH control appears to induce no significant degradation of IκBα. This is assumed to be a result of insufficient potency of TNF-α under the specific experimental conditions used. Regardless, controls that mimicked the influence of $CO_2$ on extracellular and intracellular pH resulted in IκBα degradation that was not observed under conditions of elevated $CO_2$ alone. These findings are supportive of the hypothesis that the $CO_2$-mediated inhibition of NF-κB signalling is a result of suppressed canonical activation which, in turn, is caused by an inhibition of IκBα degradation.

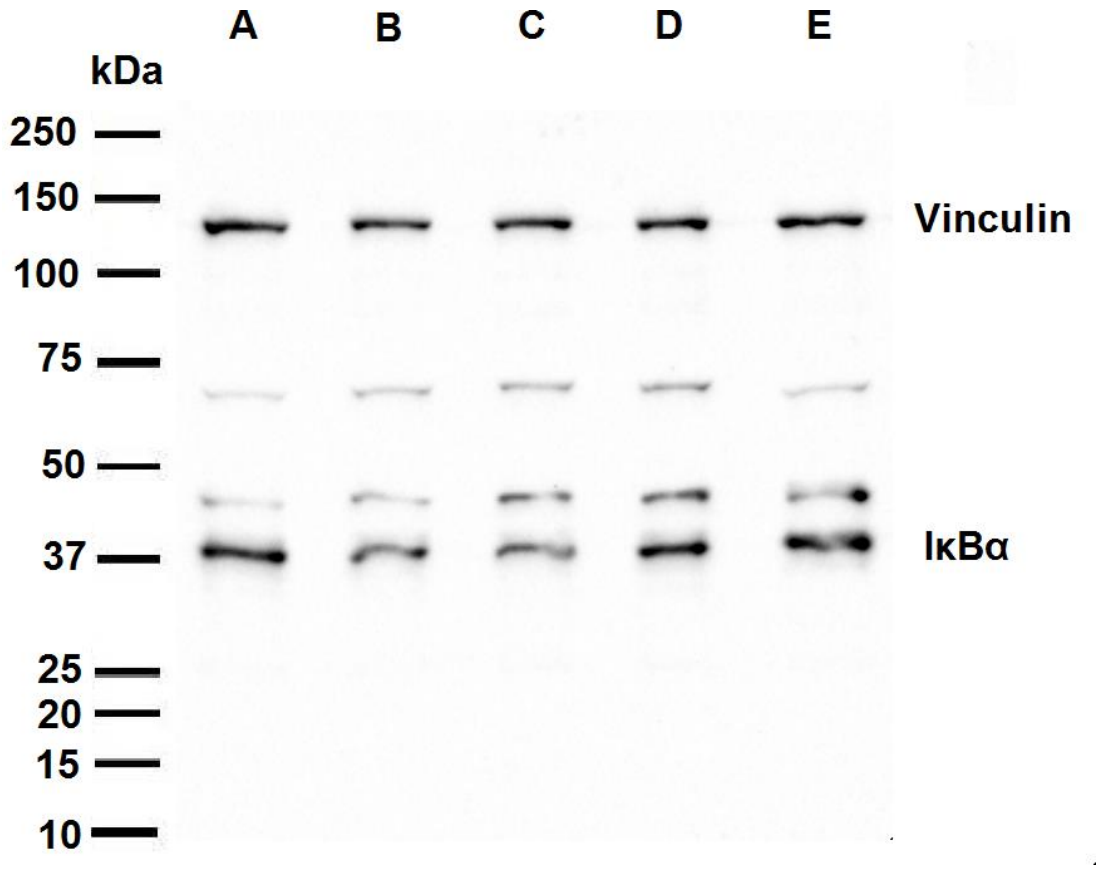


**Figure 4-7 The effect of $CO_2$ on IκBα degradation. Western blot displaying IκBα (36 kDa) and vinculin loading control (124 kDa) signal intensity. Culture treatment: A (10% $CO_2$ + 100 ng/mL TNF-α), B (5% $CO_2$ + extracellular pH control + 100 ng/mL TNF-α), C (5% $CO_2$ + intracellular pH control + 100 ng/mL TNF-α), D (5% $CO_2$ + 100 ng/mL TNF-α) and E (5% $CO_2$). All treatments were 3 h in duration.**

Further replicates are required to confirm this finding. To facilitate this, the assay must be developed to enhance the degradation of IκBα at 5% $CO_2$. Optimising the potency of TNF-α on IκBα degradation would enable the direct effect of $CO_2$ to be determined more easily. In order to strengthen the impact of TNF-α on IκBα degradation, a time-course assay was utilised. This would enable the determination of an optimum duration for which TNF-α should be exposed to cells to induce the greatest degree of IκBα degradation. Alternatively, inducing IκBα degradation could have been optimised through increasing the concentration of TNF-α. However, this is not a reasonable solution due to both cost and the likely adverse effect it would have on cell viability. Moreover, increasing the concentration of TNF-α beyond 100 ng/mL would likely elicit no impact due to a limited number of receptors per cell. 100 ng/mL TNF-α likely exceeded the ligand-receptor saturation point.

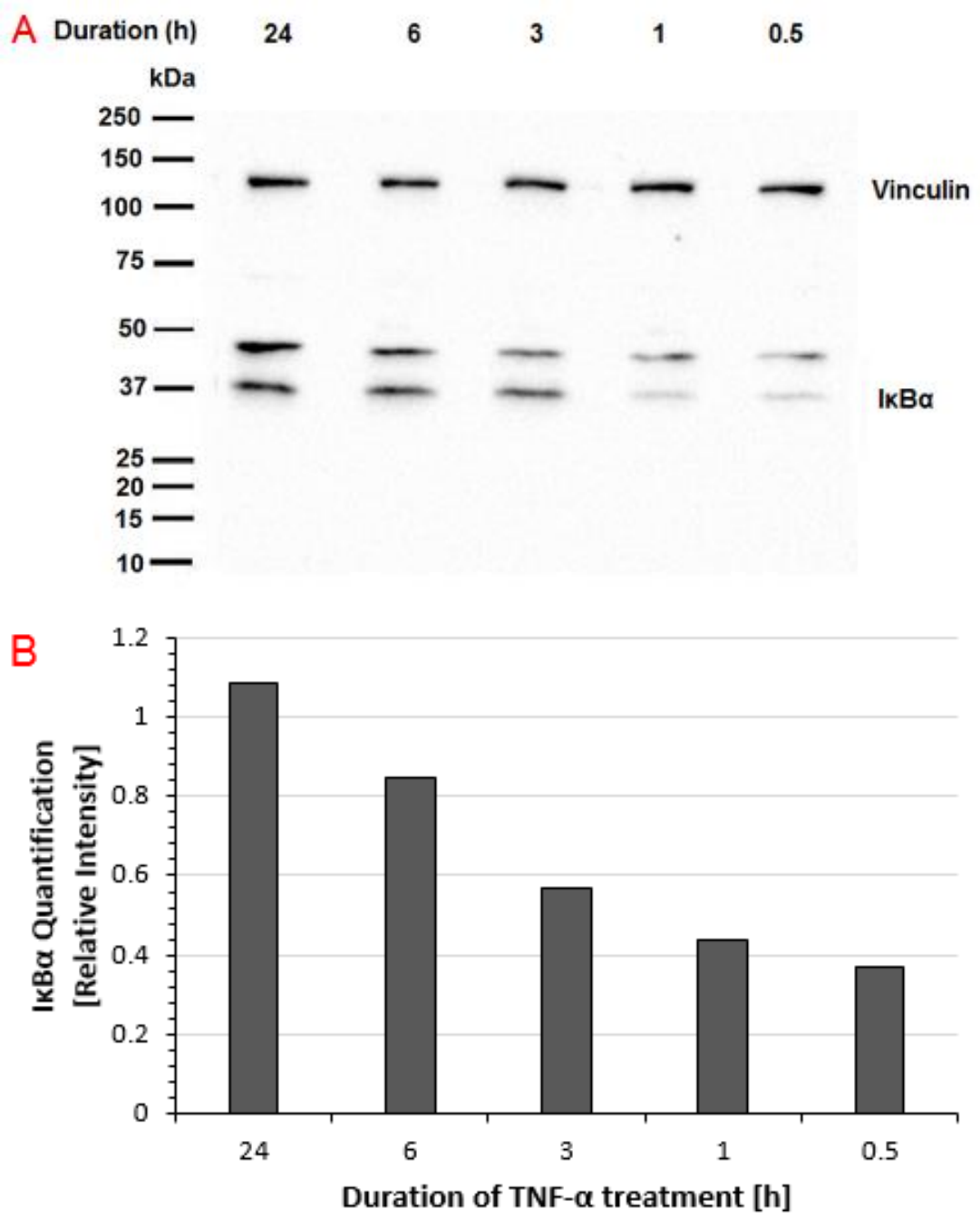


**Figure 4-8 The effect of 100 ng/mL TNF-α treatment duration on the degradation of IκBα. A: Western blots displaying IκBα (36 kDa) and vinculin loading control (124 kDa) signal intensity. B: Quantified and normalised data from Western blot (A). Relative Intensity is a calculated ratio between the IκBα signal and the vinculin loading control signal.**

The results of the TNF-α time-course assay on IκBα degradation are shown in Figure 4-8. This data indicates that 0.5 h of TNF-α treatment induces the most significant degradation of IκBα, as shown by the lowest signal intensity. A limitation of this assay lies in the lack of a 0 h treatment control. In future

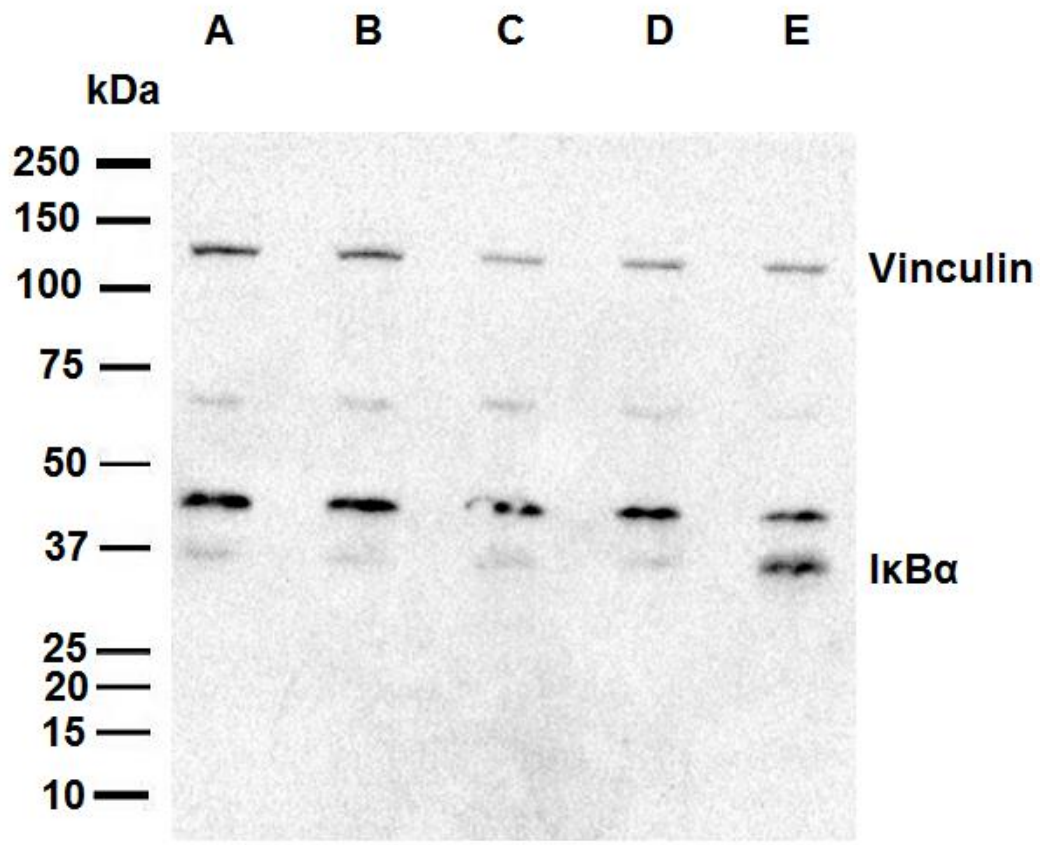


**Figure 4-9 The effect of $CO_2$ on 0.5 h TNF-α treatment-induced degradation of IκBα. Western blot displaying IκBα (36 kDa) and vinculin loading control (124 kDa) signal intensity. Culture treatment: A (10% $CO_2$ + 100 ng/mL TNF-α), B (5% $CO_2$ + extracellular pH control + 100 ng/mL TNF-α), C (5% $CO_2$ + intracellular pH control + 100 ng/mL TNF-α), D (5% $CO_2$ + 100 ng/mL TNF-α) and E (5% $CO_2$). All treatments were 0.5 h in duration.**

studies, utilisation of a 0 h treatment control would provide a useful insight into the effect of TNF-α on IκBα degradation.

Following this result, the effect of $CO_2$ on IκBα degradation was examined using only a 0.5 h duration of TNF-α treatment. It was posited that due to the increased potency of TNF-α on the degradation of IκBα, the effect of $CO_2$ on this process would be more apparent.

The result of this assay is shown in Figure 4-9. Having established the optimum incubation time for TNF-α treatment, a significant degradation of IκBα was observed. However, in this assay, the effect of 10% $CO_2$ had diminished and did not inhibit the degradation of IκBα. One possible explanation for this is that, due to the short treatment duration of 0.5 h, there was insufficient time for the complete gassing of cell media used. As a result, the increased concentration

of $CO_2$ would be unable to induce any changes within the cellular environment. Further experiments would require a pre-treatment of cells at 10% $CO_2$ for 18 h to allow full gassing of the sample prior to the treatment with TNF-α.

## 4-4 Conclusions

This chapter has investigated the relationship between $CO_2$ and activation of the NF-κB signalling pathway in association with the significance of the hypothesised role of the ubiquitin K48 residue. The results obtained showed an inhibitory effect of 10% $CO_2$ in comparison to 5% $CO_2$ on NF-κB signalling, through the utilisation of a reporter cell line. Furthermore, the importance of the ubiquitin K48 residue was duly illustrated: upon replacing this lysine with an arginine via a K48R ubiquitin mutant, an inhibitory effect on NF-κB signalling, similar to that mediated by $CO_2$, was observed. This infers that the inhibitory effect achieved by $CO_2$ is potentially a result of an induced modification of the ubiquitin K48 residue functionality.

Moreover, this chapter provided insight into the mechanism of $CO_2$-mediated inhibition of NF-κB signalling. The effect of increased $CO_2$ on the degradation of IκBα, a member of the family of molecules that inhibit NF-κB signalling via the canonical mechanism, was examined. This work indicated that $CO_2$ mediates the inhibition of IκBα degradation; this finding is, in turn, suggestive that the $CO_2$-mediated suppression of NF-κB signalling is achieved by inhibition of canonical activation, a result of decreased degradation of IκBα.

To support and develop the findings presented in this chapter, a number of further validation experiments are required. Replicates of the $CO_2$-mediated inhibition of IκBα degradation will be essential in order to confirm the findings stated in this chapter, facilitated by the implementation of the remainder of the conditions as described here. Additionally, it is vital to the integrity of the findings gleaned in this chapter to examine the functional importance of ubiquitin's six other lysine residues in the $CO_2$-mediated inhibition of NF-κB signalling, in order to better our understanding of whether this process is regulated exclusively by the K48 residue of ubiquitin.

# Chapter 5: Conclusions and future work

## 5-1 Conclusions

The development of a novel technique to trap carbamylated proteins under physiologically relevant conditions has provided a ground-breaking platform for the identification of proteins whose functions are regulated by $CO_2$ (Linthwaite *et al*., 2018). Furthermore, proteomic screenings have enabled the detection of carbamate formation on the K48 residue of ubiquitin (Linthwaite, 2017). The findings discussed in this thesis provide insight into the relationship between $CO_2$ and ubiquitin, and the effect of $CO_2$ on ubiquitin K48-regulated processes, specifically the NF-κB signalling pathway.

The functional significance of the ubiquitin K48 residue in particular has been highlighted on account of its supposed involvement in signalling for the selective degradation of intracellular proteins via the 26S proteasome; this process has been demonstrated to be dependent upon polyubiquitination at this site (Mallette and Richard, 2012). This thesis, has, indeed, demonstrated that under conditions of physiologically high concentrations of $CO_2$, an inhibition of K48-linked polyubiquitination can be observed, independent of pH. Leading from this, it was hypothesised that an inhibition of K48-linked polyubiquitination would elicit an inhibition of protein degradation, resulting in an accumulation of protein within the cell. While investigating this hypothesis demonstrated that $CO_2$ mediates no observable effect on gross cellular protein content, it was further speculated that $CO_2$ may mediate an accumulation of proteins at an individual level, most likely those regulated directly by K48-linked polyubiquitin-dependent degradation.

Additionally, this thesis examined the potential role of $CO_2$ as a mediator of the NF-κB signalling pathway in the context of its relationship with ubiquitin. Utilisation of a reporter cell line demonstrated a $CO_2$-mediated inhibition of NF-κB signalling. Furthermore, overexpression of a K48R ubiquitin mutant resulted in the inhibition of NF-κB signalling similar to that mediated by $CO_2$. From this, it was posited that the $CO_2$-mediated inhibition of NF-κB signalling is a result of an induced modification of the ubiquitin K48 residue function. Previous studies have highlighted the importance of K48-linked

polyubiquitination in signalling for the selective degradation of IκBα, a member of the family of molecules that inhibit NF-κB signalling via the canonical mechanism (Ohtake *et al*., 2016). It was thus hypothesised that the $CO_2$-mediated inhibition of NF-κB signalling was a result of inhibited degradation of IκBα. This work provided supporting evidence for this hypothesis and demonstrated a $CO_2$-mediated inhibition of IκBα degradation.

Ultimately, the work presented in this thesis is supportive of the proposed overarching hypotheses. The findings here indicate that under conditions of physiologically high $CO_2$ concentrations, increased carbamate formation inhibits polyubiquitination at the ubiquitin K48 residue. Moreover, the inhibition of K48-linked polyubiquitination as a result of carbamylation elicits a reduction in the K48-linked polyubiquitination-dependent selective degradation of IκBα. This, in turn, results in an increase in the sequestration of NF-κB dimers within the cytoplasm, and the suppression of canonical NF-κB signalling activation.

## 5-2 Future work

While the work presented in this thesis provides significant insight into the relationship between $CO_2$ and ubiquitin in the context of NF-κB signalling, a number of limitations to this study, as well as areas for future research, are apparent.

One limitation of the work described here is that this project has focused entirely on the function of the ubiquitin K48 residue in the relationship between $CO_2$ and ubiquitin-driven processes. In order to validate the findings presented within this thesis, it is important to identify whether carbamylation of ubiquitin's six other lysine residues can and does occur under physiological conditions and whether, if so, this impacts the regulation of NF-κB signalling by ubiquitin. This possibility could be explored through the transfection and overexpression of additional ubiquitin mutant constructs in cells; more specifically, constructs containing inert substitution mutations at the lysine residues of interest, thus eliminating the potential for carbamate formation.

Further important aspects for consideration in subsequent validation experiments are the potential effects of $CO_2$ on processes upstream of polyubiquitination. The findings presented in this thesis indicate that the effects mediated by $CO_2$ are a result of direct inhibition of K48-polyubiquitination. However, the phosphorylation of certain proteins has been demonstrated to be crucial to their ubiquitination (Laney and Hochstrasser, 1999). Moreover, the phosphorylation-induced K48-linked polyubiquitination-dependent degradation of IκB has been demonstrated to induce canonical activation of the NF-κB signalling pathway (Shih *et al*., 2010). It is therefore vital for the integrity of the findings presented here to demonstrate that $CO_2$ does not mediate its effects at the level of protein phosphorylation or above. This possibility could be examined through investigating the relationship between $CO_2$ and protein phosphorylation via Western blot.

Another avenue for future work is to investigate the physiological effect of $CO_2$ on other molecular components involved in the NF-κB signalling pathway. While this work focused primarily on the degradation of IκBα, examining the effect of $CO_2$ on the abundance of other proteins involved in regulation of NF-

κB signalling may aid our elucidation of the relationship between $CO_2$ and ubiquitin in NF-κB signalling.

# Chapter 6: Bibliography


Alkalay, I., Yaron, A., Hatzubai, A., Orian, A., Ciechanover, A. and Ben-Neriah, Y. (1995). Stimulation-dependent IκBα phosphorylation marks the NF-κB inhibitor for degradation via the ubiquitin-proteasome pathway. *Proceedings of the National Academy of Sciences*, 92:10599-10603.

Bedford, L., Paine, S., Sheppard, P., Mayer, R. and Roelofs, J. (2010). Assembly, structure, and function of the 26S proteasome. *Trends in Cell Biology*, 20:391-401.

Blombach, B., and Takors, R. (2015). $CO_2$-intrinsic product, essential substrate, and regulatory trigger of microbial and mammalian production processes. *Frontiers in Bioengineering and Biotechnology*, 3:108-108.

Chen, F. and Ghosh, G. (1999). Regulation of DNA binding by Rel/NF-κB transcription factors: structural views. *Oncogene*, 18:6845-6852.

Chonghaile, M., Higgins, B. and Laffey, J. (2005). Permissive hypercapnia: role in protective lung ventilatory strategies. *Current Opinion in Critical Care*, 11:56-62.

Cook, Z. (2012). The influence of carbon dioxide on cellular cyclic adenosine monophosphate. Doctoral thesis, Durham University.

Costello, R., Deegan, P., Fitzpatrick, M. and McNicholas, W. (1997). Reversible hypercapnia in chronic obstructive pulmonary disease: A distinct pattern of respiratory failure with a favorable prognosis. *The American Journal of Medicine*, 102:239-244.

Cummins EP, Oliver KM, Lenihan CR, Fitzpatrick SF, Bruning U, Scholz CC, Slattery C, Leonard MO, McLoughlin P & Taylor CT (2010). NF-κB links $CO_2$ sensing to innate immunity and inflammation in mammalian cells. *The Journal of Immunology*, 185:4439–4445.

Dev, A & Iyer, S & Razani, Bahram & Cheng, G. (2011). NF-κB and innate immunity. *Current Topics in Microbiology and Immunology*, 349: 115-143.

Dunn (1994). Autophagy and related mechanisms of lysosome-mediated protein degradation. *Trends in Cell Biology*, 4:139-143.

Freund, M. and Carol, B. (1964). Factors affecting haemocytometer counts of sperm concentration in human semen. *Reproduction*, 8:149-155.

Frommer, W. B. (2010). CO(2)mmon Sense. *Science,* 327:275-276.

Fuller, S. J., Gaitanaki, C. J., & Sugden, P. H. (1989). Effects of increasing extracellular pH on protein synthesis and protein degradation in the perfused working rat heart. *Biochemical Journal*, 259:173–179.

Gadeholt, H. (2009). Counting of cells in urine. *Acta Medica Scandinavica*, 183:9-16.

Goldberg, A. and St. John, A. (1976). Intracellular Protein Degradation in Mammalian and Bacterial Cells: Part 2. *Annual Review of Biochemistry*, 45:747-804.

Goodenough, Daniel A., and David L. Paul (2009). “Gap Junctions.” *Cold Spring Harbor Perspectives in Biology*, 1:a002576-a002576.

Gutknecht, J., Bisson, M., and Toesteson, F. (1977). Diffusion of carbon dioxide through lipid bilayer membranes. Effects of carbonic anhydrase, bicarbonate and unstirred layers. *Journal of General Physiology*, 69:779-794.

Haas AL., Siepmann, TJ. (1997). Pathways of ubiquitin conjugation. *Journal of Federation of American Societies for Experimental Biology*, 11:1257-1268.

Hampe, E. M., and Rudkevich, D. M. (2003). Exploring reversible reactions between $CO_2$ and amines. *Tetrahedron,* 59:9619-9625.

Hayden, M. and Ghosh, S. (2012). NF-κB, the first quarter-century: remarkable progress and outstanding questions. *Genes & Development*, 26:203-234.

Helenius, I., Krupinski, T., Turnbull, D., Gruenbaum, Y., Silverman, N., Johnson, E., Sporn, P., Sznajder, J. and Beitel, G. (2009). Elevated $CO_2$ suppresses specific Drosophila innate immune responses and resistance to bacterial infection. *Proceedings of the National Academy of Sciences*, 106:18710-18715.

Hershko, A., and Ciechanover, A. (1998). The ubiquitin system. *Annual Review of Biochemistry*, 67:425-479.

Hetherington, A. M., and Raven, J. A. (2005). The biology of carbon dioxide. *Current Biology,* 15:R406-R410 3.

Hoesel, B. and Schmid, J. (2013). The complexity of NF-κB signaling in inflammation and cancer. *Molecular Cancer*, 12:86.

Horiuchi, T., Mitoma, H., Harashima, S., Tsukamoto, H. and Shimoda, T. (2010). Transmembrane TNF-α: structure, function and interaction with anti-TNF agents. *Rheumatology*, 49:1215-1228.

Hsia, C. C. W. (1998). Respiratory function of hemoglobin. *New England Journal of Medicine,* 338:239-248.

Huang, H., Jeon, M., Liao, L., Yang, C., Elly, C., Yates, J. and Liu, Y. (2010). K33-linked polyubiquitination of T cell receptor-ζ regulates proteolysis-independent T cell signaling. *Immunity*, 33:830.

Jimenez-Morales, D., Adamian, L., Shi, D., and Liang, J. (2014). Lysine carboxylation: unveiling a spontaneous post-translational modification. Acta Crystallographica Section D: *Biological Crystallography*, 70:48-57.

Joshi, H. M., and Tabita, F. R. (1996). A global two component signal transduction system that integrates the control of photosynthesis, carbon dioxide assimilation, and nitrogen fixation. *Proceedings of the National Academy of Sciences,* 93:14515-14520 2.

Karin, M. (1999a). How NF-κB is activated: the role of the IκB kinase (IKK) complex. *Oncogene*, 18:6867-6874.

Karin, M. (1999b). The beginning of the end: IκB kinase (IKK) and NF-κB activation. *The Journal of Biological Chemistry*, 274:27,342.

Keogh, C., Scholz, C., Rodriguez, J., Selfridge, A., von Kriegsheim, A. and Cummins, E. (2017). Carbon dioxide-dependent regulation of NF-κB family members RelB and p100 gives molecular insight into $CO_2$-dependent immune regulation. *The Journal of Biological Chemistry*, 292:11561-11571.

Khalifah, R. (1973). Carbon dioxide hydration activity of carbonic anhydrase: paradoxica consequences of the unusually rapid catalysis. *Proceedings of the National Academy of Sciences,* 70:1986- 1989.

Kilmartin, J.V., Fogg, J., Luzzana, M., and Rossiber.L (1973). Role of α-amino groups of α and β chains of human hemoglobin in oxygen-linked binding of carbon-dioxide. *The Journal of Biological Chemistry,* 248:7039-7043.

Laffey, J.G., Honan, D., Hopkins, N., Hyvelin, J.M., Boylan, J.F., and McLoughlin, P. (2004). Hypercapnic acidosis attenuates endotoxin-induced acute lung injury. *American Journal of Respiratory and Critical Care Medicine,* 169:46-56.

Laney JD, Hochstrasser M (1999). Substrate targeting in the ubiquitin system. *Cell*, 97:427–430.

Lawrence, T. (2009). The nuclear factor NF-κB pathway in inflammation. *Cold Spring Harbor Perspectives in Biology*, 1:a001651-a001651.

Li, W. and Ye, Y. (2008). Polyubiquitin chains: functions, structures, and mechanisms. *Cellular and Molecular Life Sciences*, 65:2397-2406.

Lin, B., Williams-Skipp, C., Tao, Y., Schleicher, M., Cano, L., Duke, R. and Scheinman, R. (1999). NF-κB functions as both a proapoptotic and antiapoptotic regulatory factor within a single cell type. *Cell Death & Differentiation*, 6:570-582.

Lindskog, S. (1997). Structure and mechanism of carbonic anhydrase. *Pharmacology & Therapeutics*, 74:1-20

Linthwaite, V. (2017). Development of a technology for the discovery of protein carbamates. PhD thesis, Durham University.

Linthwaite, V., Janus, J., Brown, A., Wong-Pascua, D., O'Donoghue, A., Porter, A., Treumann, A., Hodgson, D. and Cann, M. (2018). The identification of carbon dioxide mediated protein post-translational modifications. *Nature Communications*, 9: 3092.

Lorimer, G. (1979). Evidence for the existence of discrete activator and substrate sites for $CO_2$ on ribulose-1,5-bisphosphate carboxylase. *The Journal of Biological Chemistry*, 254:5599-5601.

Lorimer, G., and Miziorko, H. (1980). Carbamate formation on the e-amino group of a lysyl residue as the basis for the activation of ribulosebisphosphate carboxylase by $CO_2$ and Mg2+. *Biochemistry,* 19:5321-5328.

Mallette, F. and Richard, S. (2012). K48-linked ubiquitination and protein degradation regulate 53BP1 recruitment at DNA damage sites. *Cell Research*, 22:1221-1223.

Manna, S. and Ramesh, G. (2004). Interleukin-8 induces nuclear transcription factor-κB through a TRAF6-dependent pathway. *Journal of Biological Chemistry*, 280:7010-7021.

Marhong, J. and Fan, E. (2014). Carbon dioxide in the critically ill: too much or too little of a good thing? *Respiratory Care*, 59:1597-1605.

Mathes, E., O'Dea, E., Hoffmann, A. and Ghosh, G. (2008). NF-κB dictates the degradation pathway of IκBα. *The European Molecular Biological Organization Journal*, 27:1357-1367.

Matthew, J., Morrow, J., Wittebort, R., and Gurd, F. (1977). Quantitative determination of carbamino adducts of α and β chains in human adult hemoglobin in presence and absence of carbon monoxide and 2,3-diphosphoglycerate. *The Journal of Biological Chemistry,* 252:2234-2244.

Meigh, L., Cook, D., Zhang, J., and Dale, N. (2015). Rational design of new NO and redox sensitivity into connexin26 hemichannels. *Open Biology,* 5:9.

Meigh, L., Greenhalgh, S. A., Rodgers, T. L., Cann, M. J., Roper, D. I., and Dale, N. (2013). $CO_2$ directly modulates connexin 26 by formation of carbamate bridges between subunits. *Elife,* 2:01213.

Miziorko H.M (1979). Ribulose-1,5-biphosphate carboxylase. Evidence in support of the existence of distinct $CO_2$ activator and $CO_2$ substrate sites. *The Journal of Biological Chemistry,* 254:270-2.

Napetschnig J, Wu H. (2013). Molecular basis of NF-κB signaling. *Annual Review of Biophysics*, 42:443-68.

Ohtake, F., Saeki, Y., Ishido, S., Kanno, J. and Tanaka, K. (2016). The K48-K63 branched ubiquitin chain regulates NF-κB signaling. *Molecular Cell*, 64:251-266.

Osborn, L., Kunkel, S. and Nabel, G. (1989). Tumor necrosis factor α and interleukin 1 stimulate the human immunodeficiency virus enhancer by activation of the nuclear factor κB. *Proceedings of the National Academy of Sciences*, 86:2336-2340.

O'Toole, D., Hassett, P., Contreras, M., Higgins, B., McKeown, S., McAuley, D., O'Brien, T. and Laffey, J. (2009). Hypercapnic acidosis attenuates pulmonary epithelial wound repair by an NF-κB dependent mechanism. *Thorax*, 64:976-982.

Plemper RK, Wolf DH (1999). Retrograde protein translocation: Eradication of secretory proteins in health and disease. *Trends in Biochemical Sciences,* 24:266–270.

Pronobis, M., Deuitch, N. and Peifer, M. (2016). The Miraprep: A protocol that uses a miniprep kit and provides maxiprep yields. *Public Library of Science ONE*, 11:e0160509.

Raines, C. A. (2003). The Calvin cycle revisited. *Photosynthesis Research,* 75:1-10.

Sadowski, M., Suryadinata, R., Tan, A., Roesley, S. and Sarcevic, B. (2011). Protein monoubiquitination and polyubiquitination generate structural diversity to control distinct biological processes. *International Union of Biochemistry and Molecular Biology Life*, 64:136-142.

Salinas, M., Rosas, J., Iborra, J., Manero, H. and Pascual, E. (1997). Comparison of manual and automated cell counts in EDTA preserved synovial fluids. Storage has little influence on the results. *Annals of the Rheumatic Diseases*, 56:622-626.

Schwartz AL., Ciechanover, A. (1992). Ubiquitin-mediated protein modification and degradation. *American Journal of Respiratory Cell and Molecular Biology,* 7:463-468.

Senftleben, U., Cao, Y., Xiao, G., *et al*. (2001). Activation by IKKα of a second, evolutionary conserved, NF-κB signaling pathway. *Science*, 293:1495–1499.

Serasanambati, M. and Chilakapati, S. (2016). Function of nuclear factor κB (NF-κB) in human diseases – a review. *South Indian Journal of Biological Sciences*, 2:368.

Shih, V., Tsui, R., Caldwell, A. and Hoffmann, A. (2010). A single NF-κB system for both canonical and non-canonical signaling. *Cell Research*, 21:86-102.

Siebenlist, U., Franzoso, G., and Brown, K. (1994). Structure, regulation and function of NF-κB. *Annual Review of Cell and Developmental Biology*, 10:405–455.

Siegel, M. And Sisler, H. (1963). Inhibition of protein synthesis in vitro by cycloheximide. *Nature*, 200:675-676.

Stec, B. (2012) Structural mechanism of RuBisCO activation by carbamylation of the active site lysine. *Proceedings of the National Academy of Sciences*, 109:18785-18790.

Sun S, Ley S (2008). New insights into NF-κB regulation and function. *Trends in Immunology*, 29:469–478.

Sun, S. (2010). Non-canonical NF-κB signaling pathway. *Cell Research*, 21:71-85.

Supuran, C. T., Scozzafava, A., and Casini, A. (2003). Carbonic anhydrase inhibitors. *Medicinal Research Reviews,* 23:146-189.

Takeshita K, Suzuki Y, Nishio K, Takeuchi O, Toda K, Kudo H, Miyao N, Ishii M, Sato N, Naoki K, Aoki T, Suzuki K, Hiraoka R & Yamaguchi K (2003). Hypercapnic acidosis attenuates endotoxin-induced nuclear factor κB activation. *American Journal of Respiratory Cell and Molecular Biology,* 29:124–132.

Terrier, P., and Douglas, D. J. (2010). Carbamino group formation with peptides and proteins studied by mass spectrometry. *Journal of the American Society for Mass Spectrometry*, 21:1500-1505.

Tornatore, L., Thotakura, A., Bennett, J., Moretti, M. and Franzoso, G. (2012). The nuclear factor κB signaling pathway: integrating metabolism with inflammation. *Trends in Cell Biology*, 22:557-566.

Vandegriff, K., Benazzi, L., Ripamonti, M., Perrella, M., Tellier, Y., Zegna, A., and Winslow, R. (1991). Carbon dioxide binding to human hemoglobin cross-linked between the α chains. *The Journal of Biological Chemistry*, 266:2697-2700.

Wilkinson, KD. (2000). Ubiquitin and deubiquitination: Targeting of proteins for degradation by the proteasome. *Seminars in Cell & Development Biology*, 11:141-148.